Environmental Science Advances

ROYAL SOCIETY OF CHEMISTRY

PAPER

View Article Online
View Journal | View Issue

Cite this: *Environ. Sci.: Adv.*, 2024, **3**, 448

Transboundary transport of air pollution in eastern Canada†

Robin Stevens,[a] Charles Poterlot,[a] Nicole Trieu,[ab] Henry Alejandro Rodriguez[a] and Patrick L. Hayes *[a]

We assess the GEOS-Chem chemical transport model against observations from the Quebec Air Quality Monitoring Network (RSQAQ) for carbon monoxide (CO), nitrogen oxides (NO_X; nitrogen oxide (NO) and nitrogen dioxide (NO_2)), fine particles having a diameter of less than 2.5 μm ($PM_{2.5}$), ozone (O_3), sulphur dioxide (SO_2), and elemental carbon (EC), a component of $PM_{2.5}$ known to have effects on both human health and climate. These pollutants have lifetimes that span from hours to weeks, allowing them to cross national borders and affect air quality far from their emission sites. We then investigate the sources of air pollution in Quebec through two complementary methods: back trajectory analysis using potential source contribution function (PSCF) and chemical transport modelling using GEOS-Chem. We perform three sensitivity studies with GEOS-Chem to determine the contributions from three source regions (Quebec, the rest of Canada, and the United States) to the concentrations of each of the investigated pollutants in Quebec. The PSCF calculations show that southern Quebec (local sources), the east coast of the United States, and southeastern Ontario are associated with days of high concentrations of several pollutants. Depending on the season, southern Quebec is associated with high concentrations of NO_X, SO_2, and CO; the east coast of the United States with high concentrations of $PM_{2.5}$, NO_X, O_3, and CO; and southeastern Ontario with high concentrations of $PM_{2.5}$ and EC. The GEOS-Chem results reveal that anthropogenic emissions from Quebec contribute the greatest amount (53%, 58%, 30%, and 44%) to concentrations of NO_X, SO_2, $PM_{2.5}$, and EC in Quebec. Anthropogenic emissions from the US were the greatest contributor to CO concentrations (11%) and summertime O_3 concentrations (17%). We find that removing all anthropogenic emissions from Quebec would reduce the fraction of the population of Quebec living in regions that exceed the recommended annual mean WHO $PM_{2.5}$ concentration threshold of 5.0 μg m^{-3} from 87.7% to about 0.0%. While an absolute cessation of anthropogenic emissions is neither feasible nor desirable, our results suggest that substantial improvements in air quality in Quebec would be possible through reductions in local emissions alone despite the strong influence of transboundary transport.

Received 2nd October 2023
Accepted 25th January 2024

DOI: 10.1039/d3va00307h

rsc.li/esadvances

Environmental significance

It is well-known that ozone, fine aerosol particles ($PM_{2.5}$), sulphur dioxide, nitrogen oxides, and carbon monoxide are harmful to human health. From 2016–2022, Montreal experienced between 21 and 43 poor air quality days per year, and air quality monitoring stations in Quebec reported from 2 to 278 "poor" air quality days in 2021. Therefore, it continues to be important to understand the sources of air pollution in Montreal and in the province of Quebec more generally. Specifically, we investigate in this study the contributions from local sources which can be addressed through local action and transboundary transport which required cooperation with other jurisdictions to address.

1. Introduction

Air pollution is well known to have harmful effects on human health.[1–4] However, the lifetimes of many common air pollutants span from days to weeks, allowing these air pollutants to cross national and sub-national borders, negatively affecting human health in other countries and even other continents than those where they were emitted.[5–10] Addressing the problem of air pollution therefore requires cooperation across jurisdictions, which should be informed by knowledge of the relationships between source emissions and atmospheric concentrations in receptor regions.

From 2016–2022, Montreal experienced between 21 and 43 poor air quality days per year, defined as days with concentrations of fine particles having a diameter of less than 2.5 μm

[a]*Department of Chemistry, Faculty of Arts and Sciences, Université de Montréal, Montréal, Québec, Canada. E-mail: patrick.hayes@umontreal.ca*

[b]*Department of Chemical Engineering & Applied Chemistry, Faculty of Applied Science & Engineering, University of Toronto, Toronto, Ontario, Canada*

† Electronic supplementary information (ESI) available. See DOI: https://doi.org/10.1039/d3va00307h

($PM_{2.5}$) greater 35 μg m^{-3}. Annual mean concentrations of $PM_{2.5}$ were 7.1 μg m^3 in Montreal in 2022, beyond the WHO air quality guideline of 5 μg m^{-3}.[11] The province of Quebec uses an Air Quality Index calculated based on the concentrations of ozone (O_3), $PM_{2.5}$, sulphur dioxide (SO_2), nitrogen oxides (NO_X; nitrogen oxide (NO) and nitrogen dioxide (NO_2)), and carbon monoxide (CO). Based on this Air Quality Index, the stations in Quebec reported from 2 to 278 "poor" air quality days in 2021.[12] Therefore, it continues to be important to understand the sources of air pollution in Montreal and in the province of Quebec more generally. Specifically, we wish to investigate in this study the contributions from local sources which can be addressed through local action and transboundary transport which required cooperation with other jurisdictions to address.

It is well known that emissions from anthropogenic sources within the US contribute to concentrations at the surface within Quebec and that air quality in Quebec is episodically influenced by biomass burning emissions in northwestern Canada.[13,14] Summertime surface-level ozone in eastern Canada has been shown to be greatest during periods of southwesterly flow.[15,16] A previous study has examined the contributions to $PM_{2.5}$ in Canada by source sector, and highlighted the importance of wildfires, transportation, and residential combustion.[17] They additionally found that sources within the US were responsible for 33% of population-weighted $PM_{2.5}$ in Central Canada, a region which includes Manitoba, Ontario, and Quebec.

Montreal constitutes a large city (metropolitan population of four million) in an otherwise rural region, located in the outflow region of the industrialized northeastern US, including the megacity of New York City. This is therefore a good region for studying the transport and transformation of urban and industrial emissions into a populated boreal region. Historically, transport of US emissions into the Quebec region has been examined closely due to concerns of acid rain,[13,18,19] but continued examination of this transboundary transport is important because of possible changes in transport with climate change,[20] historical changes in emissions,[21,22] an expanded set of pollutants of interest, expansions and improvements in monitoring,[11,23] and improvements in techniques for attributing transboundary transport, including chemical transport modelling[24–28] and back-trajectory modelling.[29–32]

We investigate several pollutants monitored by the Quebec Air Quality Monitoring Network (RSQAQ, Réseau de Surveillance de la Qualité de l'Air du Québec).[23] The data collected at the RSQAQ sites is included in the Canadian National Air Pollution Monitoring Network (NAPS) Program,[33] and those stations on the island of Montreal are operated by the city of Montreal Air Quality Monitoring Network (RSQA, Réseau de surveillance de la qualité de l'air).[11] We will describe the observational data in more detail in Section 2.1. Specifically, we investigate CO, NO_X, $PM_{2.5}$, O_3, SO_2, and elemental carbon (EC). It is well known that these pollutants can be harmful to human health.[1–4] We include EC in our analysis because it is a particularly interesting component of $PM_{2.5}$: it absorbs solar radiation and can contribute to global warming. Thus, efforts to reduce the concentration of EC will improve air quality while reducing radiative forcing leading to climate change. The distribution by sector of $PM_{2.5}$ in Canada has previously been investigated by Meng *et al.* (2019)[17] for the year 2013. In this study, we focus on a breakdown by region in order to specify the concentrations of pollutants from Quebec or outside Quebec. The years analyzed are 2014, 2015 and 2016. Quebec is Canada's largest province by size and second-largest by population and is located to the north and east of major population centers in Canada and the USA, and thus it is susceptible to receiving transboundary pollution transported by prevailing winds.

We present a general back-trajectory analysis for the province of Quebec. Calculating back trajectories is a well-established method for identifying geographic regions that are potential sources of air pollution.[7,30–32] To better explain this method, consider the calculation of a normal trajectory that advances in time. The simulation begins at a given point in space and time that would correspond to the release of a pollutant from a source (*e.g.* a factory or a smelter). From this point, the movements of the pollutant can be calculated using meteorological data, including wind direction and speed. This simulation operates over time to generate a trajectory. If it is repeated several times starting from different times, for example on subsequent days, the set of trajectories can be superimposed to make a frequency map of the path of the trajectory. To calculate a back trajectory, the simulation is built in the same way, but the calculations proceed in the opposite direction in time, compared to the normal trajectory. Thus, if the simulation begins at an observation site, the regions upwind of the site are identified.

In order to take into account the observed concentrations of pollutants, maps of the Potential Source Contribution Function (PSCF) were calculated. PSCF is a method of weighting a set of back trajectories using data from a monitoring station so that source regions that are associated with high concentrations of a pollutant at a station can be identified.[29,34,35] PSCF maps are calculated for all the pollutants specified above, *i.e.* CO, NO_X, $PM_{2.5}$, O_3, SO_2, and EC at each station. To facilitate the interpretation of the results, the PSCF maps for several stations in Quebec are averaged for each pollutant.

A complementary approach to assess transboundary transport is the use of chemical transport models. In these models, the atmosphere is divided into a three-dimensional grid based on latitude, longitude and altitude. Atmospheric processes are comprehensively simulated in three dimensions, including emissions, transport and chemistry. Such models are used to make air quality forecasts, to help develop environmental policies and for research. Since these models include emission inventories, it is possible to modify these emissions to study the impact of different sectors or regions on air pollutant concentrations. At the same time, emissions inventories may contain errors or may not accurately represent actual emissions. This is a limitation of this approach, and it is therefore desirable to combine this approach with other methods such as back trajectory calculations.

Therefore, to complement the PSCF analysis, we use the GEOS-Chem chemical transport model to simulate pollutant concentrations in Quebec for four scenarios. The first scenario

includes the emission inventories without modification. In the other scenarios, emissions were removed in Quebec, the United States or the other Canadian provinces and territories. This series of scenarios allows us to estimate the quantities of a pollutant from each of these regions. We begin with the results of the GEOS-Chem simulations to assess the transboundary input of air pollutants, and more specifically, the quantities coming from the United States or the rest of Canada (RoC). Then, back-trajectory analysis and PSCF maps are used to identify more precisely the most important source regions in the United States and Canada.

The article is organized as follows: Section 2 explains in detail the methodologies used, including the observational data (Section 2.1), the calculations to produce the back trajectories and PSCF maps (Section 2.2) and the chemical transport modelling by GEOS-Chem (Section 2.3). Section 3 presents the validation of GEOS-Chem using the observational data (Section 3.1), the assessment of transboundary input based on GEOS-Chem results (Section 3.2) and the results of the PSCF maps (Section 3.3). We compare the PSCF and chemical transport modelling results in Section 4. Finally, the conclusions of the study are summarized in Section 5.

2. Experimental methods

2.1 Observational data

The observational data used in this study was collected at stations operated by either the RSQAQ or the city of Montreal air quality monitoring network, and all of the stations participate in the NAPS program. The RSQAQ and the City of Montreal's air quality monitoring network use similar instrumentation and the same data collection and quality assurance protocols. For a complete description of the data collection methods, we refer the reader to the Ambient Air Monitoring and Quality Assurance/Quality Control Guidelines, National Air Pollution Surveillance Program.[33] For simplicity, we will refer to all observation stations as RSQAQ stations in the rest of this article.

We use the data from the RSQAQ stations for two purposes: First, to evaluate the results of the base-case GEOS-Chem simulation, and secondly, to perform the PSCF analysis. To evaluate GEOS-Chem, we use data from 2012 to 2016 inclusive. For the PSCF analysis, we focus on data for the years 2014 to 2016 inclusive, in order to avoid periods of missing data and to have a more continuous dataset. EC was measured at two stations (Tables A1 and A2†) with a frequency of one day in three or one day in six and an interval of 24 hours. All other pollutants were monitored continuously year-round and reported by the government as hourly averages. We aggregated the pollutant concentration data into monthly averages for comparison with the GEOS-Chem results, and into daily averages for the PSCF calculations. The stations used in this report to obtain data for the PSCF calculations are summarized in Table A1 and Fig. A1.† We list the stations used to evaluate GEOS-Chem in Table A2.†

Since the RSQAQ stations are positioned to monitor population exposure, the majority of the stations are in urban centers or on their outskirts. As the population of Quebec is concentrated on the shores of the St. Lawrence River which is in the south of the province, the stations are also geographically concentrated in the south of the province. However, the purpose of this study is to investigate transboundary sources of pollution. The location of the stations could therefore present some challenges for the PSCF analysis: the first is that the stations located in urban centers measure ambient pollution which is more likely to be strongly influenced by local emissions at a scale finer than that which can be resolved by the PSCF analysis, and the cross-border contribution is added to this local pollution. If the monitoring station were in a rural setting, the transboundary input would become a larger part of the total concentration, and it would therefore be easier to quantify the transboundary input and its sources. We also do not want the PSCF analysis to be dominated by sources that only affect Montreal or Québec City, where the greatest number of stations are located. To limit the influence of local emissions for stations located in urban areas and to ensure that the PSCF analysis is regionally representative, we only used data from one station in each of Montreal and Québec City in the PSCF analysis. The second problem is the sampling bias towards the south of the province due to the large number of stations concentrated in this part of the province. As the vast majority of the population of Quebec lives in the south of the province, we expect that our results will nonetheless be representative of the pollution sources that affect the majority of Quebec's population. In addition, the largest sources outside of Quebec are to the south and southwest of the province, and they are not expected to exert as large an influence on air pollutant concentrations in northern Quebec. In fact, this assumption is supported by the GEOS-Chem results presented below. Thus, as the purpose of this study is to study transboundary contributions, it is useful to have a greater number of datasets from monitoring stations near the south and southwest borders of the province.

For the evaluation of GEOS-Chem, we exclude observations from seven stations that are known to be directly downwind of large point sources (Table A3†). The model results yield pollutant concentrations averaged over the resolution of our simulations (0.5° latitude by 0.625° longitude), and thus it is impossible for the model to capture highly concentrated plumes, such as those measured at these stations. For the model evaluation, we use data from a total of 34 stations, of which 32 measure $PM_{2.5}$, 32 measure O_3, 12 measure NO_X, 8 measure SO_2, 6 measure CO, and 2 measure EC.

2.2 Back-trajectory and PSCF analysis

Several trajectory models have been developed to study atmospheric transport.[30–32] In this study, we used the Hybrid Single-Particle Lagrangian Integrated Trajectory (HYSPLIT) model developed by the National Oceanic and Atmospheric Administration (NOAA) in the United States.[30] The backward trajectories of the air masses observed at the RSQAQ stations were calculated for the period from 2014–2016 inclusive. Meteorological data from the Global Data Assimilation System (GDAS)[36] with a resolution of 1° were obtained from the NOAA website and used to carry out the simulations.

To estimate the potential locations of sources of air pollutants transported over long distances, we used the ZeFir software

package[37] to calculate PSCF maps using the back-trajectories calculated with HYSPLIT. From the HYSPLIT trajectory modelling results, the air mass movement can be represented as segments that create a trajectory describing the air movements upstream of the site. If a segment of a trajectory is in a geographical cell defined on a map, this cell will then be considered as a potential contributor of pollutants transported to the receiving site. PSCF is used to generate a probability map of cells around a monitoring site where the probability that a cell is associated with a high concentration of a pollutant is indicated. The probabilities are calculated according to eqn (1) below where n_{ij} is the total number of segments entering cell ij and m_{ij} is the number of segments entering the same cell for which the concentration of a pollutant when the trajectory arrives at the site is within the 90th percentile.

$$\mathrm{PSCF}_{ij} = \frac{m_{ij}}{n_{ij}} \quad (1)$$

The daily concentrations of pollutants at the RSQAQ sites were used in the calculations of the PSCF maps. The trajectories were calculated 5 days backwards in time and were started at a height of 500 m above ground level; this altitude was chosen to limit the effects of local topography. The domain of interest displayed in the PSCF graphs extends from 20° N to 80° N and from 40° W to 150° W. In a PSCF analysis, small values of n_{ij} can generate high PSCF probabilities with large uncertainties due to lack of data.[29,35] Therefore, to improve the visual representation of the results, a sigmoidal weighting function, $w(n_{ij})$, was applied to the PSCF_{ij} values.[38–40]

$$w = \frac{1}{1 + \mathrm{e}^{-10(x-0.5)}} \quad (2)$$

$$x = \frac{\log(n_{i,j} + 1)}{\max(\log(n_{i,j} + 1))} \quad (3)$$

Finally, there were a number of days when it was not possible to perform the PSCF analysis due to a lack of meteorological data or a lack of measurements of a pollutant. The percentages of days missing from the PSCF analysis are summarized in Tables A3–A8.†

2.3 GEOS-Chem simulations

We perform simulations using the GEOS-Chem chemical transport model (version 14.0.2, **https://doi.org/10.5281/zenodo.7383132**).[24,25] GEOS-Chem is driven by assimilated meteorology from the Modern-Era Retrospective analysis for Research and Applications, Version 2 (MERRA-2) dataset produced by the NASA Global Modeling and Assimilation Office (GMAO). We generate boundary conditions using a global simulation at 2° latitude x 2.5° longitude resolution. We then use a nested grid with 0.5° latitude × 0.625° longitude resolution, spanning 35° N to 65° N, 90° W to 50° W in order to include the full province of Quebec as well as the strong source regions of the Great Lakes region and the northeastern US. We performed simulations from 2012–2016, but we report results in Section 3.2 only from 2014–2016 for consistency with the PSCF analysis. Our simulations therefore have a spin-up period of two years for the analysis, and a spin-up period of one month for the evaluation against the RSQAQ observations. The atmosphere is resolved using 47 vertical layers from the surface to 0.01 hPa. The vertical resolution of the model is about 100 m near the surface, but it becomes coarser at higher altitudes. Biomass-burning emissions are simulated from the Global Fire Emissions Database version 4 (GFED4).[41] Anthropogenic emissions from Canada are provided by the Air Pollutant Emissions Inventory (APEI), recently processed for use in chemical transport models as described in Crippa *et al.* (2023).[21] Anthropogenic emissions from the US are provided by the National Emissions Inventory for 2016,[42] with annual scaling factors to account for changes in emissions relative to 2016. Shipping emissions are provided by the Community Emissions Data System version 2 (CEDSv2),[22] and aircraft emissions are provided by the Aviation Emissions Inventory Code (AEIC).[43,44] We use the recently developed wet particle entrainment treatment described by Luo *et al.* (2019, 2020),[27,28] which has been shown to provide better agreement with nitrate and ammonium concentrations over eastern North America.

In order to examine the sensitivity of air pollutant concentrations to transboundary transport, we perform a base-case simulation with no changes in emissions and three sensitivity simulations, each with anthropogenic emissions from a geographic region turned off. In the first sensitivity simulation (noQC), we do not allow any anthropogenic emissions within the borders of the province of Quebec. In the second simulation (noRoC), we do not allow any anthropogenic emissions within the borders of Canada, except for emissions from the province of Quebec (Rest of Canada, RoC). In the third simulation (noUS), we do not allow any anthropogenic emissions within the borders of the contiguous United States. We include emissions from shipping and aircraft within the boundaries of the specified region as anthropogenic emissions, therefore we reduce these to zero as well. We have not changed emissions from wildland fire or natural sources. We note that for the purposes of masking emissions, each model grid cell is considered to be entirely within one province or country; the resolution of the provincial or national masks is the same as the model resolution. By calculating the differences in the concentrations of air pollutants in the sensitivity simulations compared to the base-case simulation, we estimate the proportions of air pollutants in Quebec due to sources within Quebec, sources in the rest of Canada, and sources in the contiguous United States.

Despite the two complementary investigative techniques, there are still limits to our methodology. The chemical transport model results shown here rely on high-quality, spatially and temporally resolved emissions inventories. Reporting and monitoring of emissions is crucial to the creation and updating of these emissions inventories. In addition, the chemical transport model and the back trajectory analysis are dependent on the accuracy of the reanalysis meteorological data, which in turn depends in part on local meteorological monitoring.

3. Results and discussion

3.1 Evaluation of GEOS-Chem against observations for Quebec, Canada

We evaluate the results of our GEOS-Chem simulations against the observations made at the RSQAQ stations. This evaluation is summarized in Tables 1 and 2 and shown in Fig. 1–3. We use as our metrics of evaluation the Pearson's correlation coefficient (R), the mean error (ME), the normalized mean error (NME), the mean bias (MB), and the normalised mean bias (NMB), where ME, NME, MB, and NMB are defined as follows. The x_i variables indicate the model predictions and the y_i variables indicate the observed data for a given station, both as monthly averages, and N is the number of model-observation pairs:

$$\mathrm{ME} = \frac{1}{N}\sum_{i=1}^{N}|x_i - y_i| \quad (4)$$

$$\mathrm{NME} = \frac{\sum_{i=1}^{N}|x_i - y_i|}{\sum_{i=1}^{N} y_i} \times 100 \quad (5)$$

$$\mathrm{MB} = \frac{1}{N}\sum_{i=1}^{N} x_i - y_i \quad (6)$$

$$\mathrm{NMB} = \frac{\sum_{i=1}^{N}(x_i - y_i)}{\sum_{i=1}^{N} y_i} \times 100 \quad (7)$$

In order to provide a more in-depth assessment of the accuracy of GEOS-Chem regarding the spatial and temporal variations for each pollutant, we also recalculate R after averaging the model and observation data for all stations (temporal R) or after averaging these data over time for each station individually (spatial R). We do not average multiple stations within a single GEOS-Chem grid cell in agreement with previous studies that state that this artificially improves model-observations agreement.[6]

When all seasons are considered, the correlation coefficients range from 0.29 for CO to 0.76 for EC. Temporal correlation coefficients vary from 0.37 for SO_2 to 0.91 for NO_X, and spatial correlation coefficients vary from 0.11 for CO to 0.65 for $PM_{2.5}$. We note that with only two stations where EC was measured, it is not useful to calculate a spatial correlation coefficient for EC. The higher temporal correlations show that GEOS-Chem is able to reproduce the seasonal cycles of each pollutant, which is also visible in the time series comparisons presented in Fig. 3. The low spatial correlation between the GEOS-Chem results and the CO observations are partly due to the low spatial variability of the observed concentrations. Mean CO concentrations differ by less than 0.014 ppm between stations (~7%, Fig. 1c and 2c), and this small variability is less likely to be due to regional-scale differences in CO concentrations than to other factors, especially smaller scale variability that cannot be reproduced by GEOS-Chem. Furthermore, in our analysis, 3 of the 6 stations measuring CO are located in the same GEOS-Chem grid cell (Montréal – Rivière Des Prairies, Montréal – Aéroport de Montréal, and Laval – Chomedey), and the modelling results will therefore give exactly the same CO concentrations for these three stations. The same challenge exists for simulating NO_X concentrations: 5 of the 12 stations used in our analysis are in the Montreal area, and one station is in the city of Laval (Fig. 1d and 2d). These six stations are all within a single GEOS-Chem grid cell, and therefore GEOS-Chem predicts the same NO_X concentrations for all 6 stations. Similarly, 3 of the 12 stations are in the Québec City region, also covered by a single GEOS-Chem grid cell.

Table 2 Evaluation of the GEOS-Chem base-case simulation against observations from the RSQAQ stations given in Table A2 for winter (December, January and February) or summer (June, July and August). The units of ME and MB are μg m^{-3} for $PM_{2.5}$ and EC, ppm for CO, and ppb for all other species

Pollutant	Season	ME	NME [%]	MB	NMB [%]
$PM_{2.5}$ [μg m^{-3}]	Winter	2.70	34	−0.871	−11
	Summer	1.73	23	−0.421	−6
CO [ppm]	Winter	0.058	24	−0.045	19
	Summer	0.043	21	−0.029	−14
NO_X [ppb]	Winter	7.10	52	−6.93	−50
	Summer	2.95	48	−2.91	−47
SO_2 [ppb]	Winter	0.468	46	0.052	5
	Summer	0.438	82	0.223	42
O_3 [ppb]	Winter	4.49	17	4.12	15
	Summer	8.24	33	8.20	33
EC [μg m^{-3}]	Winter	0.160	30	−0.079	−15
	Summer	0.160	35	−0.154	−34

Table 1 Evaluation of the GEOS-Chem base-case simulation against observations from the RSQAQ stations given in Table A2. The units of ME and MB are μg m^{-3} for $PM_{2.5}$ and EC, ppm for CO, and ppb for all other species. Spatial R is not included for EC because it is not a meaningful statistic with only two stations

Pollutant	R	Temporal R	Spatial R	ME	NME [%]	MB	NMB [%]
$PM_{2.5}$ [μg m^{-3}]	0.55	0.73	0.65	2.03	30	−0.229	−3
CO [ppm]	0.29	0.74	0.11	0.051	24	−0.042	−20
NO_X [ppb]	0.61	0.91	0.42	4.79	50	−4.70	−49
SO_2 [ppb]	0.41	0.37	0.57	0.469	60	0.105	13
O_3 [ppb]	0.75	0.79	0.61	7.32	28	7.17	27
EC [μg m^{-3}]	0.76	0.62	—	0.137	31	−0.084	−19

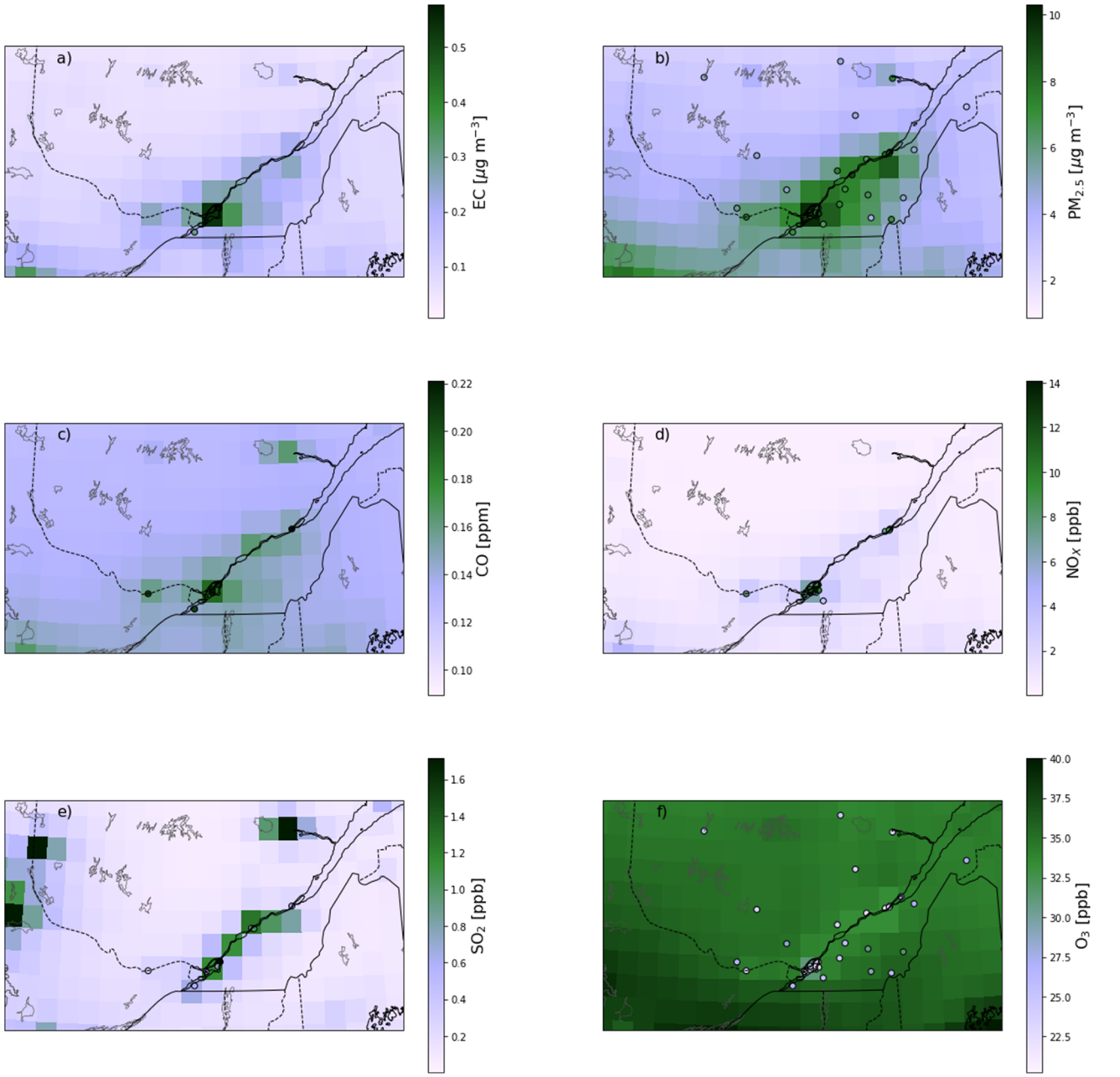

Fig. 1 Map of mean concentrations simulated by the base case GEOS-Chem simulation, with the mean concentrations at the RSQAQ stations superimposed. Values are shown for (a) EC, (b) $PM_{2.5}$, (c) CO, (d) NO_X, (e) SO_2, and (f) O_3.

There are small biases for CO and EC and a moderate bias for NO_X. There may be a contribution to the bias in NO_X concentrations from an underestimate in NO_X emissions or an overestimate of O_3 concentrations, which would lead to an overestimation of NO_X oxidation. As we will show in Section 3.2, NO_X concentrations have one of the greatest relative contributions from local sources (53.2% from sources within Quebec) of the pollutants we examine. As all but one of the stations measuring NO_X were in urban locations (Fig. 1d), the grid-cell means from GEOS-Chem would be expected to be less than the point measurements from the RSQAQ stations. Silvern *et al.* (2019)[45] previously found that GEOS-Chem underestimated NO_2 concentrations in a similar manner at the United States Environmental Protection Agency Air Quality System sites, which are mainly in urban locations. The same study found a greatly reduced low bias for GEOS-Chem NO_2 concentrations compared against observations at rural locations. Moreover, the relative interannual trend at both rural and urban locations from 2005–2017 was well reproduced by GEOS-Chem in that study. The effect of coarse resolution leading to a low bias with respect to surface observations of NO_2 has also been previously shown to affect satellite observations in a similar manner.[46–48] This model resolution effect likely also contributes to the low biases in CO and EC concentrations.

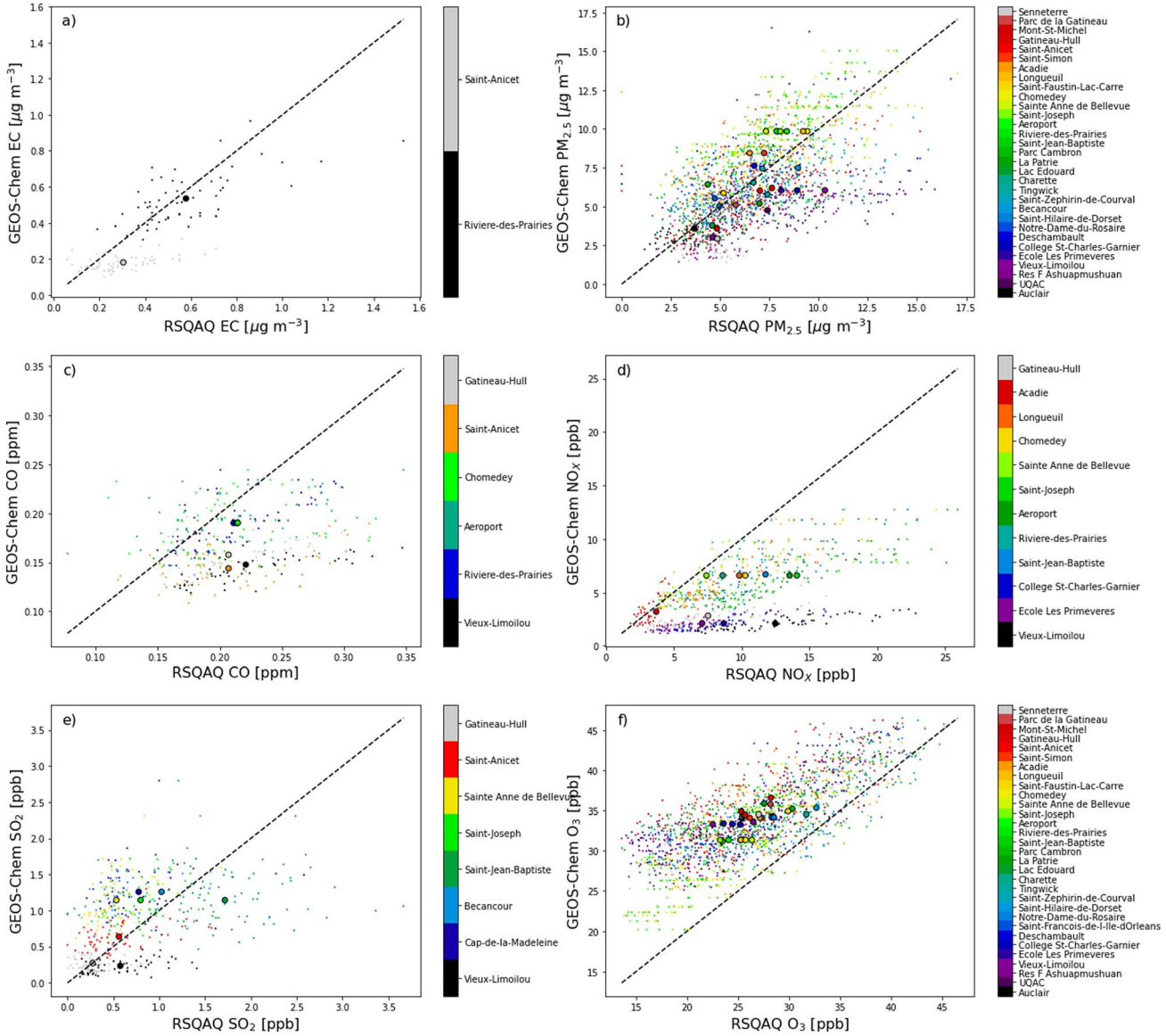

Fig. 2 Scatterplot of GEOS-Chem simulated concentrations *vs.* concentrations observed at the RSQAQ stations. Temporal averages at each station are displayed as large dots. Values are shown for (a) EC, (b) $PM_{2.5}$, (c) CO, (d) NO_X, (e) SO_2, and (f) O_3.

Conversely, the stations measuring $PM_{2.5}$ were almost evenly split between urban and rural locations (15 and 17, respectively), so the effect of model resolution on the bias would be less uniformly negative. Similar to this work, Kim *et al.* (2015)[49] found a good correlation ($R = 0.65$) for $PM_{2.5}$ concentrations when comparing against observations from US measurement networks for September and August of 2013, and that study also found a slightly negative bias of −1.4%, which is similar to our NMB of −3%, despite the finer resolution of the model (0.25° × 0.3125°) used in this previous study. The model error and model bias in $PM_{2.5}$ concentrations is greater in winter than in summer (Table 2). We will show in Section 3.2.2 (Tables 3 and 4, Fig. A10 and A11†) that GEOS-Chem predicts both a larger fraction of $PM_{2.5}$ from Quebec anthropogenic sources and a larger fraction of $PM_{2.5}$ from anthropogenic sources in general in winter *vs.* summer. It is therefore likely that there is an increased contribution from local primary sources in winter such as emissions from residential home heating. These sources are more difficult to resolve in 0.5° latitude × 0.625° longitude grid cells than secondary formation of $PM_{2.5}$, which would be more prominent in summer, and this would lead to a low model bias as discussed above for NO_X concentrations.

GEOS-Chem exhibits a positive bias in O_3 concentrations which is greater in summer and fall and smaller in winter and spring (Tables 2, A10,† Fig. 3f). Several atmospheric models (including GEOS-Chem) have been previously shown by Reidmiller *et al.* (2009) to have a summer peak in O_3 concentrations that is too late when compared to observations in Maine and Vermont, which resulted in a multi-model mean JJA mean bias of 10 ppb.[5] However, we find that the seasonal cycle in O_3 concentrations is reproduced well for Quebec, albeit with a consistently high bias that is similar to the previous work of

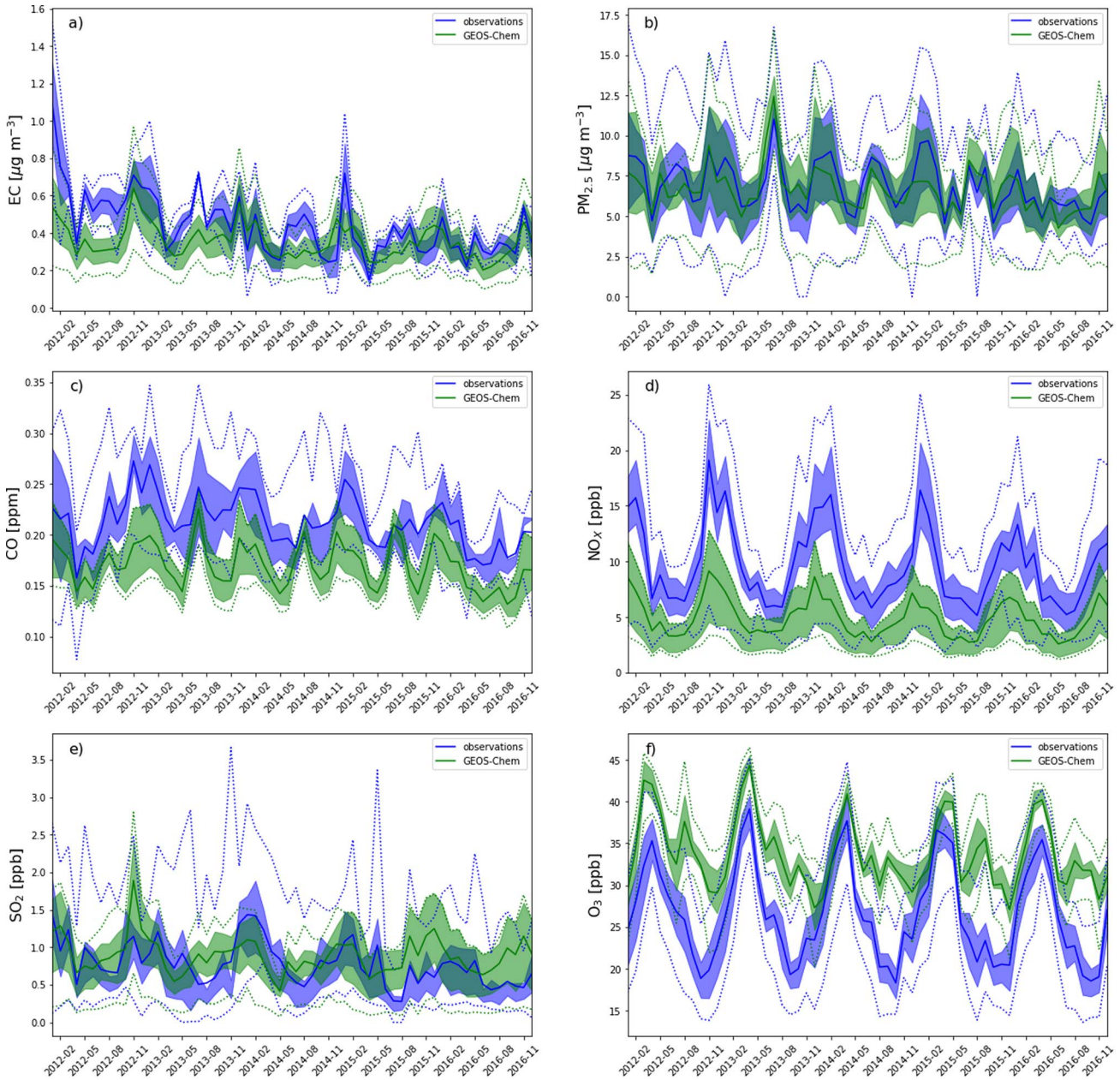

Fig. 3 Time series of pollutant concentrations averaged at RSQAQ station locations. Values simulated by GEOS-Chem are in green, while RSQAQ observations are in blue. The shaded region gives the interval between the 25th and 75th percentiles. Dotted lines indicate minimums and maximums. Values are shown for (a) EC, (b) $PM_{2.5}$, (c) CO, (d) NO_X, (e) SO_2, and (f) O_3.

Table 3 Relative differences between the sensitivity simulations and the base-case simulation, spatially averaged over a region that encompasses the locations of the RSQAQ stations and the large population centres (45° N to 49° N, 78.75° W to 68.75° W)

	2014–2016			DJF			JJA		
	noQC	noRoC	noUS	noQC	noRoC	noUS	noQC	noRoC	noUS
O_3	0.9%	2.4%	11.1%	−2.2%	−0.4%	4.3%	4.5%	5.2%	16.6%
NO_X	53.2%	14.1%	25.4%	48.3%	15.9%	35.2%	56.6%	11.5%	13.2%
SO_2	57.6%	26.7%	18.3%	55.5%	28.6%	25.1%	59.7%	25.9%	9.7%
CO	5.6%	2.5%	11.2%	7.1%	3.5%	15.1%	4.3%	1.9%	7.9%
$PM_{2.5}$	30.2%	13.5%	27.9%	38.7%	15.1%	34.1%	18.3%	10.7%	19.6%
EC	43.8%	14.9%	32.8%	45.3%	14.9%	36.8%	37.4%	14.6%	25.6%

Table 4 Absolute differences between the sensitivity simulations and the base case simulation, spatially averaged over a region that encompasses the locations of the RSQAQ stations and the large population centres (45° N to 49° N, 78.75° W to 68.75° W). The units of $PM_{2.5}$ and EC are given as μg m^{-3} and all other species are given as ppb

	2014–2016			DJF			JJA		
	noQC	noRoC	noUS	noQC	noRoC	noUS	noQC	noRoC	noUS
O_3	0.296	0.832	3.789	−0.733	−0.138	1.441	1.368	1.601	5.099
NO_X	0.395	0.104	0.188	0.577	0.190	0.420	0.242	0.049	0.057
SO_2	0.118	0.055	0.038	0.147	0.076	0.067	0.102	0.044	0.016
CO	7.441	3.364	14.982	10.219	4.952	21.557	6.070	2.695	11.063
$PM_{2.5}$	1.166	0.523	1.080	1.457	0.569	1.285	0.841	0.492	0.897
EC	0.043	0.015	0.032	0.055	0.018	0.045	0.035	0.014	0.024

Reidmiller *et al.* (2009). One possible source of this bias is the difference in vertical sampling between the model and the observations: the lowest model vertical level is centered at 65 m above ground level, while the observations were typically sampled at about 2 m above ground level. Previous studies have attempted to correct for this bias, and have calculated that this effect is responsible for a 3 ppb overestimation in southeastern US maximum daily 8 h average (MDA8) surface ozone[50] and approximately 0.5 μg m^{-3} in continental US $PM_{2.5}$.[51] The method that was used to correct for this bias assumes no surface emissions of the species being corrected, and thus is only applicable to O_3 and the secondary components of $PM_{2.5}$, not to any of the other pollutants discussed in this study. Additionally, the low model bias in NO_X concentrations may contribute to the high O_3 bias where NO_X titration occurs, specifically in urban locations in wintertime. We performed a correlation analysis between the model biases in O_3 concentrations and the model biases in NO_X concentrations at stations that measure both pollutants, and we found spatial correlation coefficient of −0.76: The stations with higher mean NO_X concentrations have greater underestimations in NO_X concentrations, and also greater overestimations of mean O_3 concentrations (Fig. A2,† also compare Fig. 1d and f, 2d and f). This spatial correlation was strongest in winter (spatial $R = -0.89$) when NO_X titration is expected to occur, and weakest in summer (spatial $R = -0.15$).

In summary, GEOS-Chem can reproduce the observed concentrations and variability of $PM_{2.5}$, O_3 and EC. The observed variability of NO_X is well reproduced, but the concentrations simulated by GEOS-Chem have a negative bias. This bias is likely due in part to small-scale variations in NO_X concentrations that are not relevant to the regional-scale analysis that we will present in Section 3.2. Small-scale variations also likely impact CO spatial correlation and bias. The model performs somewhat less well in predicting SO_2 and CO concentrations, but it is still useful in assessing transboundary

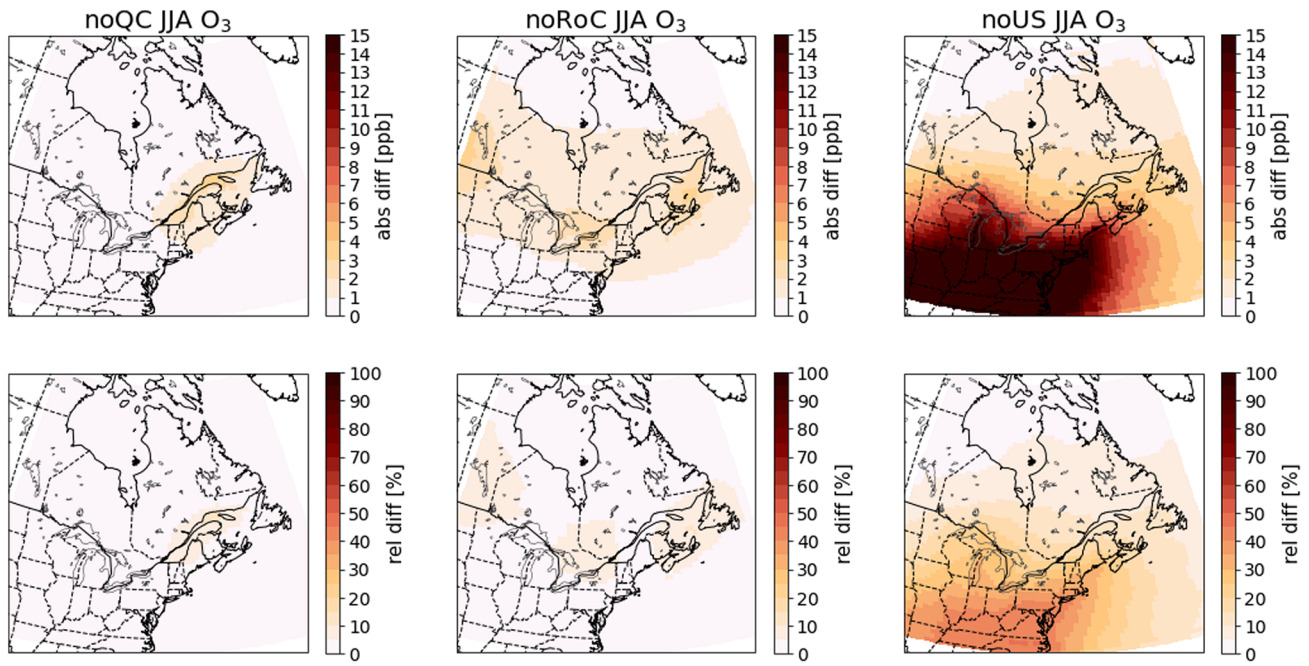

Fig. 4 Differences in summer (JJA) surface O_3 concentrations between the sensitivity simulations and the base-case simulation. Absolute differences are shown in the top row and relative differences in the bottom row. The three columns show the results of the noQC (left), noRoC (center) and noUS (right) sensitivity simulations.

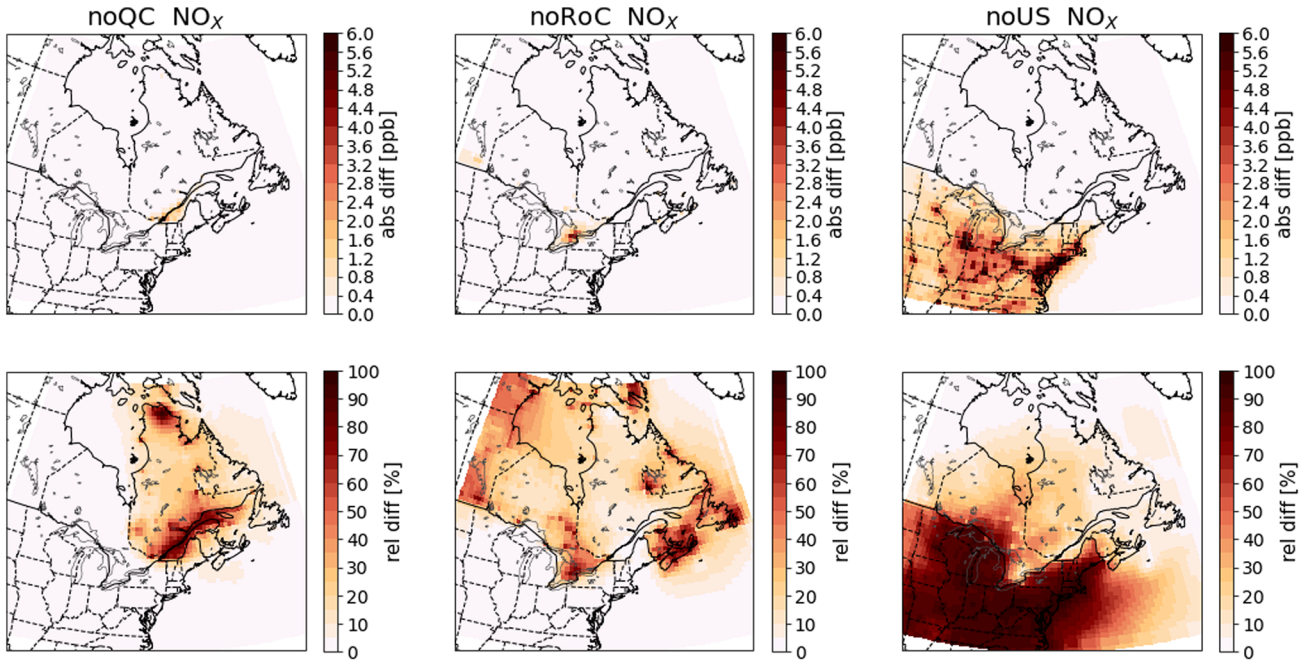

Fig. 5 Differences in annual mean surface NO_X concentrations between the sensitivity simulations and the base case simulation. Absolute differences are shown in the top row and relative differences in the bottom row. The three columns show the results of the noQC (left), noRoC (center) and noUS (right) sensitivity simulations.

transport, albeit with larger uncertainties. Further work is needed to improve simulations of these species with GEOS-Chem for Quebec, possibly by using higher resolution model runs that can be performed with the high performance version of GEOS-Chem.[26]

Finally, we note that in our analysis, we will be examining the differences between two sets of simulations. Therefore, many potential sources of error, including uncertainties in natural emissions, long-range transport from outside of North America, and model meteorology would affect the

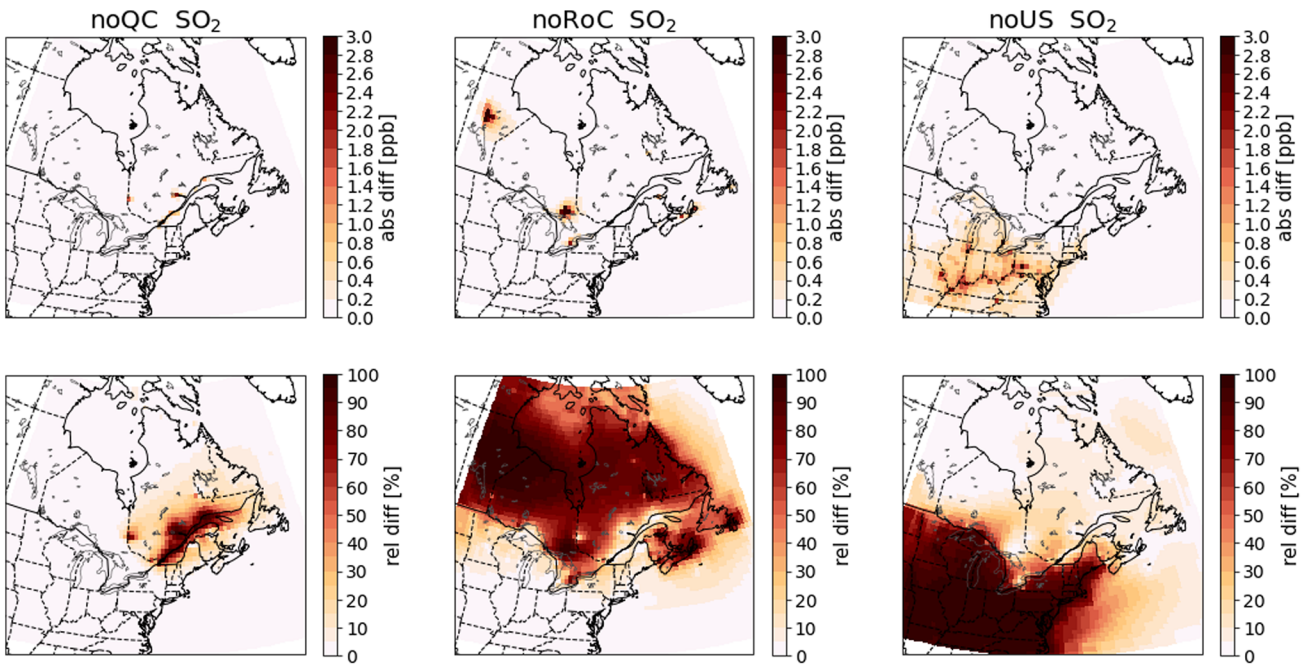

Fig. 6 Differences in annual mean surface SO_2 concentrations between the sensitivity simulations and the base-case simulation. Absolute differences are shown in the top row and relative differences in the bottom row. The three columns show the results of the noQC (left), noRoC (center) and noUS (right) sensitivity simulations.

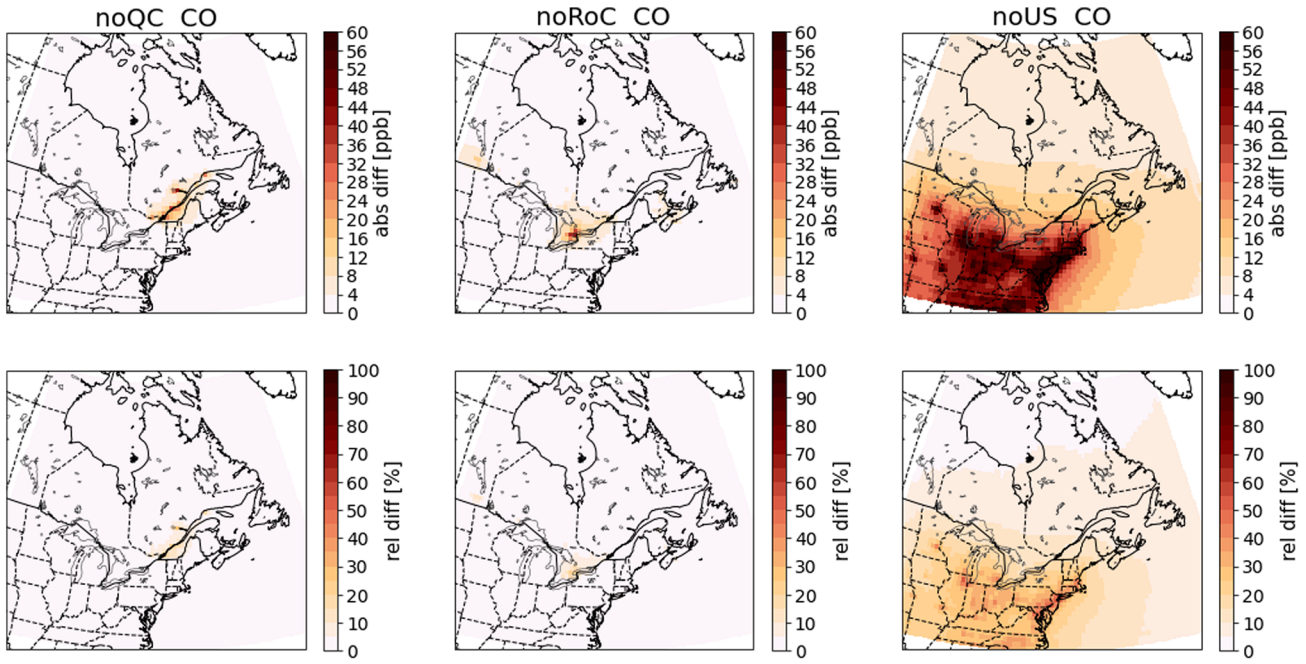

Fig. 7 Differences in annual mean surface CO concentrations between the sensitivity simulations and the base case simulation. Absolute differences are shown in the top row and relative differences in the bottom row. The three columns show the results of the noQC (left), noRoC (center) and noUS (right) sensitivity simulations.

results of all simulations in the same way. We therefore expect that results based on the differences between simulations will be more robust than the predictive power of the base-case simulation.

3.2 Apportionment of pollutants to emissions in Quebec, the RoC, and the US

To evaluate the contributions from emissions in Quebec, the RoC, and the US to O_3, NO_X, SO_2, CO, $PM_{2.5}$, and EC, the results

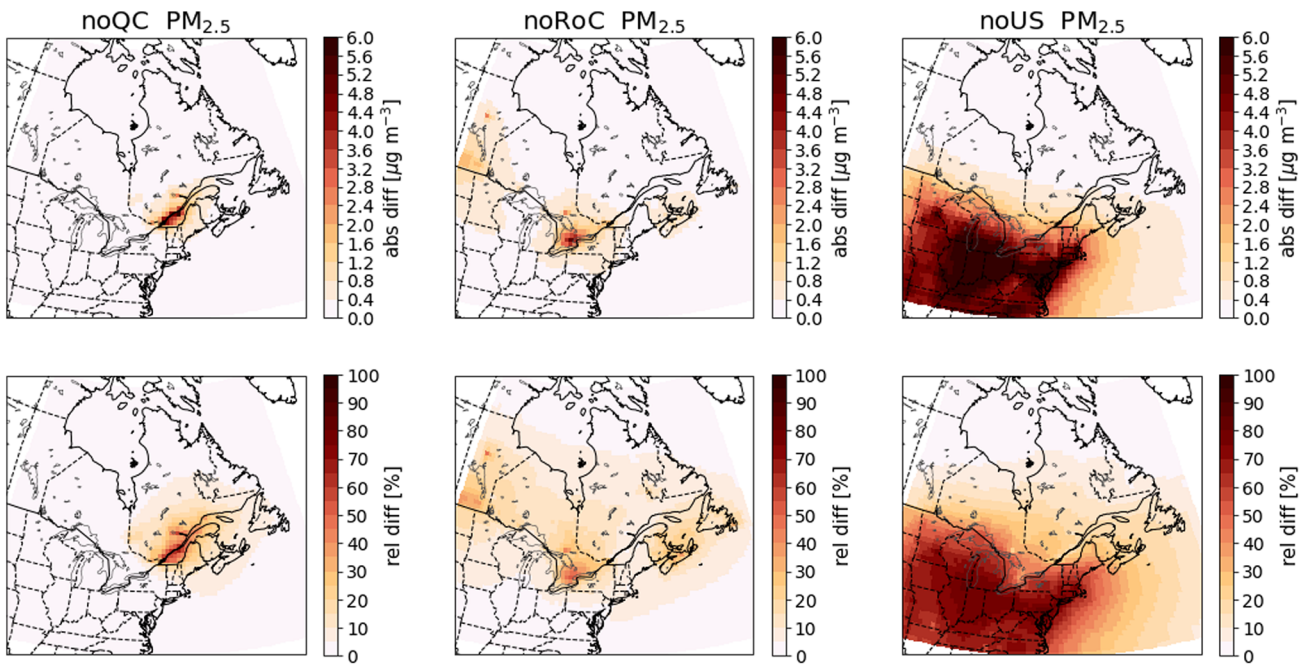

Fig. 8 Differences in annual mean surface $PM_{2.5}$ concentrations between the sensitivity simulations and the base-case simulation. Absolute differences are shown in the top row and relative differences in the bottom row. The three columns show the results of the noQC (left), noRoC (center) and noUS (right) sensitivity simulations.

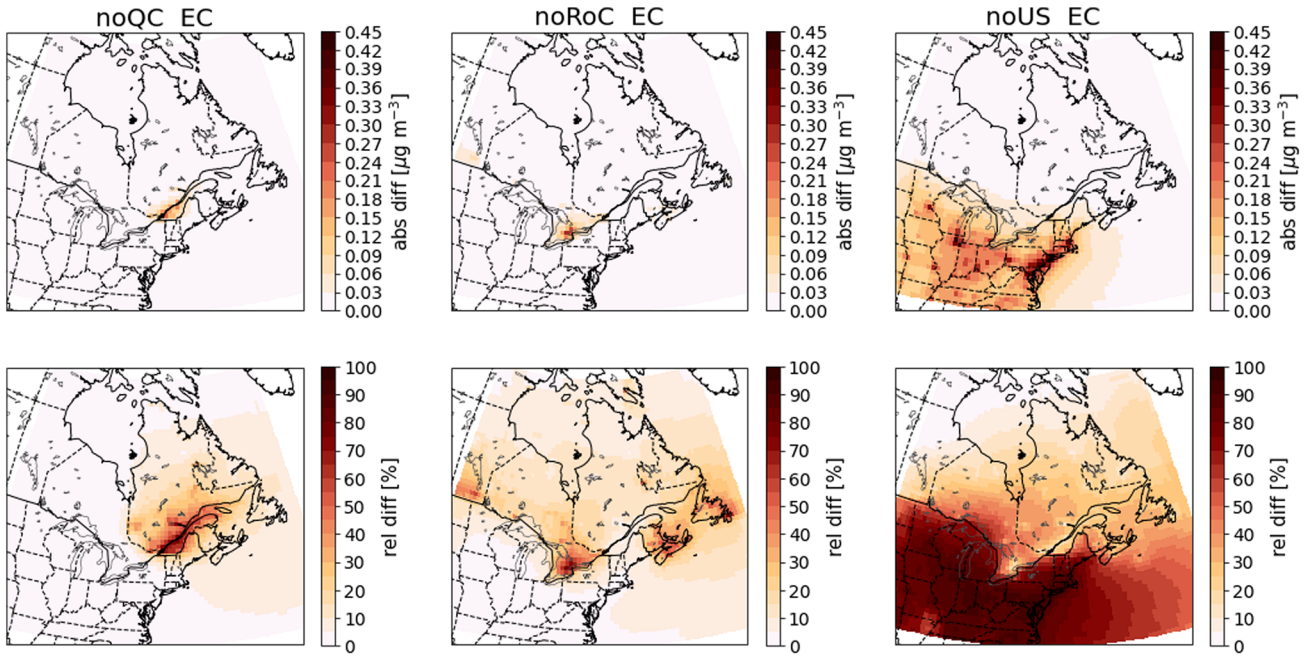

Fig. 9 Differences in annual mean surface EC concentrations between the sensitivity simulations and the base-case simulation. Absolute differences are shown in the top row and relative differences in the bottom row. The three columns show the results of the noQC (left), noRoC (center) and noUS (right) sensitivity simulations.

Table 5 Percentage of the area or population of Quebec exceeding the CAAQS or WHO concentration thresholds in each simulation when averaged from 2012–2016

Threshold	Base case	noQC	noRoC	noUS
Area exceeding 8.8 μg m^{-3}	1.5%	1.3%	1.3%	1.3%
Area exceeding 5.0 μg m^{-3}	7.3%	3.5%	6.4%	4.7%
Population exceeding 8.8 μg m^{-3}	39.0%	0.0%	0.0%	0.0%
Population exceeding 5.0 μg m^{-3}	87.7%	0.0%	85.8%	66.8%

from the GEOS-Chem simulations are plotted as differences between the sensitivity simulations and the base-case simulation. Specifically, for each pollutant, we average the surface concentrations annually, and over either winter (DJF) or summer (JJA) of the 2014–2016 period. Fig. 4–9 show the absolute differences (base case – sensitivity case) and the relative differences (base case – sensitivity case)/(base case) in the mean concentrations. We show the summer mean for O_3 and annual means for all other pollutants. Figures for winter and summer for all pollutants are given in the ESI (Fig. A2–A13†). To facilitate comparison of the GEOS-Chem modelling results with the PSCF results shown in Sect. 3.3, we also show in Tables 3 and 4 the relative and absolute differences averaged over 45° N to 49° N, 78.75° W to 68.75° W, a region that encompasses all of the RSQAQ sampling stations used in the PSCF analysis. We note that as many of the RSQAQ sampling stations have been placed with the objective of determining the exposure of Quebec's population to atmospheric pollution, this region also encompasses the area where the vast majority of Quebec's population is located, including the cities of Montreal and Québec City.

As expected, most pollutants show the greatest differences in concentrations over the emissions regions that are set to zero in the sensitivity simulations, and absolute differences in concentrations are larger in the southern part of Quebec where the RSQAQ stations are located than in the northern parts of the province. Additionally, when emissions from one of the three regions are removed, differences in concentrations are typically larger during winter than summer. One contributing factor to this seasonal cycle is the seasonal cycle in boundary layer heights: due to warmer surface temperatures, boundary layer heights are greater in summer than in winter. The same mass of pollution is therefore diluted in a larger vertical layer in summer than winter. Another factor is the concentration of oxidants which will react with certain pollutants such as SO_2. Concentrations of oxidants are generally higher in summer, which decreases the lifespan and therefore the accumulation of these pollutants. Therefore, in the absence of seasonal differences in emissions or horizontal transport, we would expect higher concentrations of any primary pollutant in winter than in summer.

3.2.1 Gaseous pollutants. Ozone presents a notable exception to the seasonal patterns described in the previous paragraph (Fig. 4 and A3†): anthropogenic emissions decrease O_3 over strong emissions regions in the winter due to NO_X titration, but increase O_3 in the summer. More specifically in Quebec, anthropogenic emissions from Quebec decrease O_3 in winter for the region of Montreal, indicating that O_3 production is limited by volatile organic compound (VOC) concentrations, and a decrease in O_3 of up to 6.8 ppb is simulated. It should be noted, however, that exceedances of the 8 hours O_3 standard are generally not observed in winter. In contrast, in summer O_3 appears to be NO_X-limited

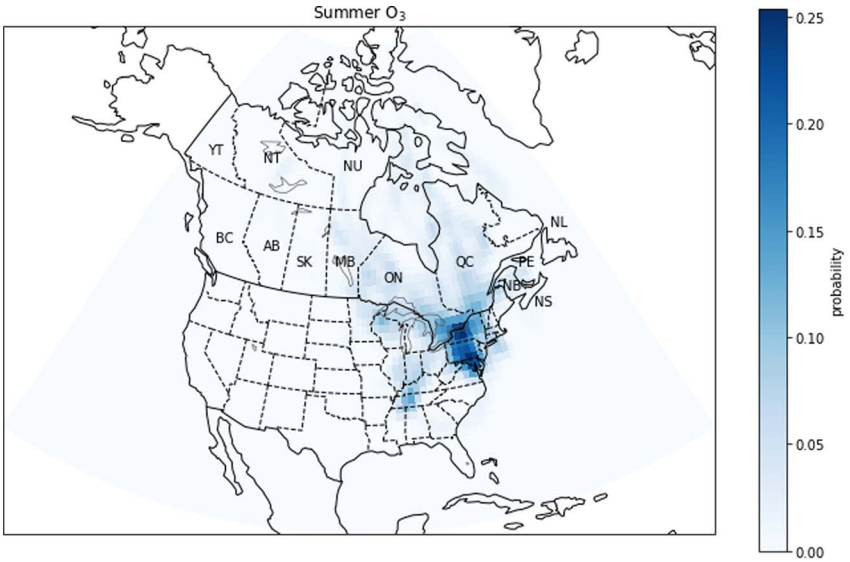

Fig. 10 Summer probability source contribution function map calculated using the O_3 measurements. Canadian provinces and territories are labeled by postal abbreviation. NL: Newfoundland and Labrador, PE: Prince Edward Island, NS: Nova Scotia, NB: New Brunswick, QC: Quebec, ON: Ontario, MB: Manitoba, SK: Saskatchewan, AB: Alberta, BC: British Columbia, YT: Yukon, NT: Northwest Territories, NU: Nunavut.

and Quebec emissions lead to an increase in ozone between 1 and 4 ppb in the vicinity of the St. Lawrence River, including New Brunswick and Maine. Zeroing emissions from the Rest of Canada (RoC) results in a similar magnitude effect on all of Quebec south of about 55° N. Emissions from the US increase summer O_3 concentrations by at least 1 pbb for most of Quebec, and the magnitude of the difference increases to 7 ppb at the US-Quebec border. We find that US emissions have the greatest impact on summer O_3 concentrations of the three regions investigated, not only within Quebec, but for nearly the entire domain included in our simulations.

We note that while the maximum O_3 concentrations occur in spring, the effect of anthropogenic emissions on O_3 concentrations is most positive in summer and most negative in winter, suggesting that the spring maximum and fall minimum are features of the background O_3 in this region, due to either long-range transport from outside of North America, biogenic emissions, or stratospheric–tropospheric exchange. This also suggests that anthropogenic emissions in this region have the effect of shifting the annual O_3 maximum later in the year, as has been discussed in other studies.[52,53]

NO_X and SO_2 are reactive gases with a relatively short lifetime in the atmosphere. Therefore, the absolute differences in NO_X and SO_2 concentrations between the simulations are largely constrained to the source regions (Fig. 5 and 6). Within Quebec, only the noQC simulation shows differences in NO_x greater than 0.8 ppb, and these are observed in the region surrounding the St. Lawrence River. In this simulation, the annual mean difference in NO_X concentrations in Montreal reaches almost 5.4 ppb. Similarly, the greatest changes to SO_2 concentrations in Quebec are seen in the noQC simulation, with a small number of grid cells showing increases due to Quebec emissions of more than 1 ppb, likely due to strong point sources. The impacts of emissions removal extends over a larger region in winter than summer (compare Fig. A4 with Fig. A5 and Fig. A6 with Fig. A7†), because oxidation of NO_X and SO_2 is slower due to lower oxidant concentrations during this season. For example, emissions from the United States increase NO_X concentrations by 0.4 ppb up to a latitude of 47° N in winter, but they do not yield increases greater than 0.4 ppb beyond the Quebec-US border in summer. In winter, emissions from outside of Quebec do not increase concentrations of SO_2 within Quebec by more than 0.2 ppb, except emissions from the RoC close to the Ontario-Quebec border.

Carbon monoxide has a longer lifetime than either NO_X or SO_2, and therefore increases in CO persist further from the source regions than for NO_X or SO_2 (Fig. 7). This allows emissions from the US to enhance CO concentrations by more than 4 ppb throughout all of Quebec. Of the three emissions regions investigated in this study, emissions from the US have the greatest effect on CO concentrations in Quebec, except close to large emissions sources in Quebec. In these locations, the effect of Quebec emissions exceeds the effect of US emissions. However, we note that unlike NO_x and SO_2, the GEOS-Chem simulations indicate that CO in Eastern Canada, including Quebec at the scale resolved by GEOS-Chem is not primarily due to North American anthropogenic emissions. This is in agreement with a previous source apportionment study, which showed that Asian anthropogenic CO emissions contributed more to CO concentrations within Quebec than North American anthropogenic CO emissions in April of 2008.[54]

3.2.2 Particulate matter. Next, we will discuss particulate matter and EC, an important component of particulate matter. From Fig. 8, it can be seen that transboundary transport strongly influences $PM_{2.5}$ concentrations in Quebec. Spatial patterns are similar in summer and winter, but with reduced magnitudes of change in summer (compare Fig. A10 and A11†). During winter, local anthropogenic emissions increase $PM_{2.5}$ concentrations by

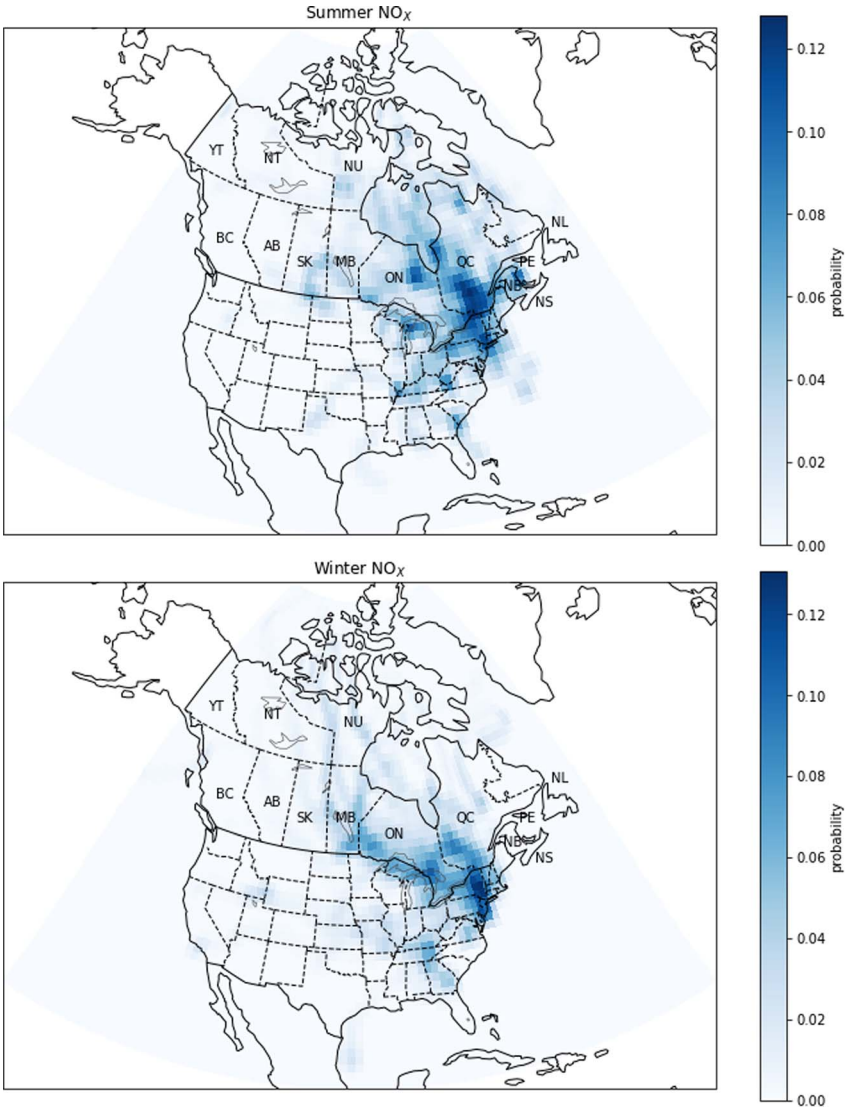

Fig. 11 Probability source contribution function maps calculated using the NO_X measurements. Top figure: summer probabilities. Bottom figure: winter probabilities. Canadian provinces and territories are labeled by postal abbreviation. NL: Newfoundland and Labrador, PE: Prince Edward Island, NS: Nova Scotia, NB: New Brunswick, QC: Quebec, ON: Ontario, MB: Manitoba, SK: Saskatchewan, AB: Alberta, BC: British Columbia, YT: Yukon, NT: Northwest Territories, NU: Nunavut.

more than 5.0 μg m^{-3} along the St. Lawrence River, but the maximum increase from this source is only 4.0 μg m^{-3} in summer. Emissions from the RoC increase concentrations by more than 0.4 μg m^{-3} as far east as the Quebec-Maine border in both seasons. Emissions from the United States increase concentrations by 0.4 μg m^{-3} further north and further east within Quebec than the RoC emissions in all seasons. The US contribution to concentrations increases towards the Canada-US border, reaching 3.2 μg m^{-3} at the border in winter and 2.4 μg m^{-3} in summer.

An important consideration in this study is that summertime EC concentrations can be influenced by outdoor biomass combustion emissions, especially from forest fires. As we have not included these biomass combustion emissions in the anthropogenic emissions that we modify in the sensitivity simulations, the EC concentration derived from outdoor biomass combustion emissions will be identical in all simulations. In regions where outdoor biomass combustion is the main source of EC, the differences in its concentration after removal of anthropogenic emissions will be small. This effect is responsible for the small relative differences in EC concentrations in northern Quebec, especially during summer (Fig. 9, A12†). This consideration applies to all species emitted from biomass combustion, including CO (Fig. 7), if their emissions from biomass combustion are predominant. As shown in Fig. 9, the differences in EC between the base case simulation and the sensitivity simulations has a spatial pattern similar to that observed for $PM_{2.5}$. Emissions from Quebec cause increases in EC that are largest along the St. Lawrence River, while emissions from the RoC do not produce increases within Quebec greater than 0.03 μg m^{-3}. Emissions from the United States produce increases greater than 0.03 μg m^{-3} as far north as 47° N.

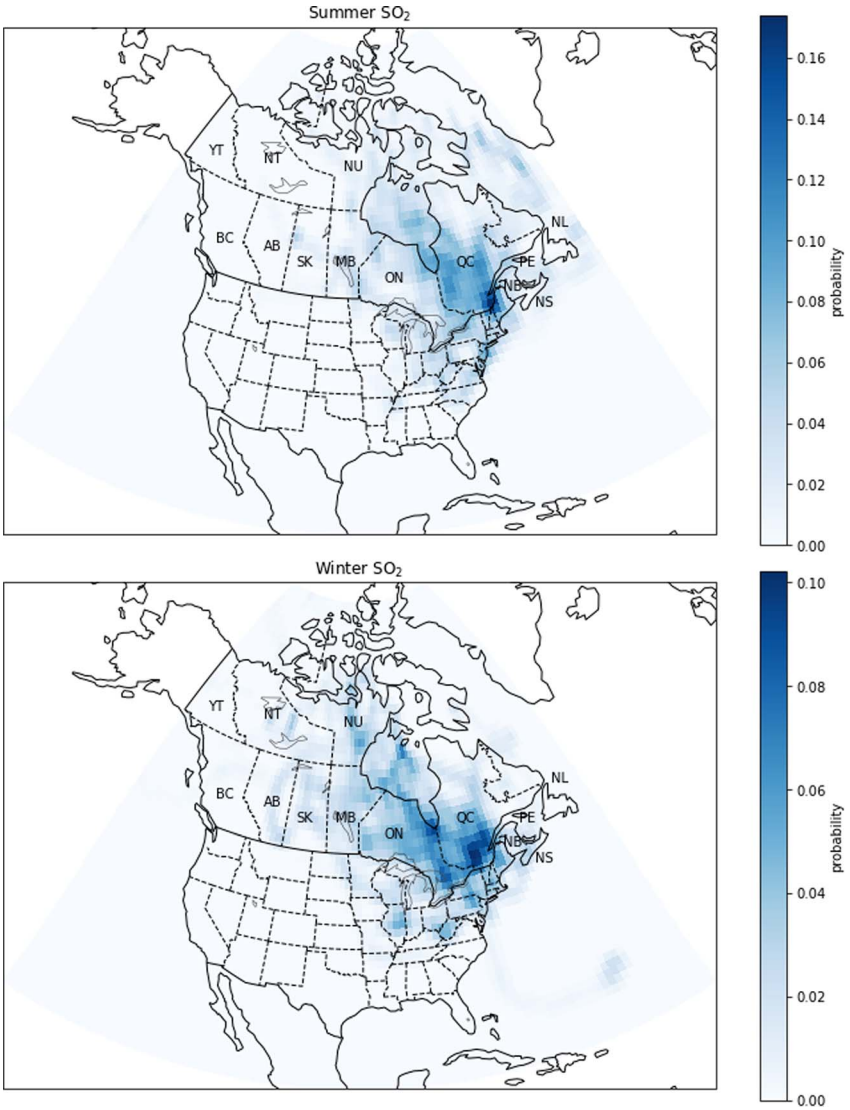

Fig. 12 Probability source contribution function maps calculated using the SO_2 measurements. Top figure: summer probabilities. Bottom figure: winter probabilities. Canadian provinces and territories are labeled by postal abbreviation. NL: Newfoundland and Labrador, PE: Prince Edward Island, NS: Nova Scotia, NB: New Brunswick, QC: Quebec, ON: Ontario, MB: Manitoba, SK: Saskatchewan, AB: Alberta, BC: British Columbia, YT: Yukon, NT: Northwest Territories, NU: Nunavut.

We further examine the importance of emissions from the three regions to $PM_{2.5}$ concentrations in Quebec by calculating the area of Quebec that exceeds the annual average concentration thresholds recommended for 2020 by the Canadian Ambient Air Quality Standards (CAAQS) (8.8 μg m^{-3})[55] or the World Health Organization (WHO) air quality guidelines (5 μg m^{-3})[56] in each simulation. The results are summarized in Table 5, and the values for individual years are in Tables A12 and A13.†

We supplement this analysis by using 10 km data for the 2016 Canadian population[57] to calculate the Quebec population living in geographic cells where $PM_{2.5}$ concentrations exceed thresholds of 8.8 μg m^{-3} or of 5.0 μg m^{-3}. The percentages of the population of Quebec living in the geographic cells that exceed these thresholds are presented in Table 5, and the values for each year are given in Tables A14 and A15.† In the base-case simulation, the areas covering 39.0% and 87.7% of the total population of Quebec exceed respectively 8.8 or 5 μg m^{-3}. By removing the emissions from either Quebec, the RoC or the United States, the population of Quebec where the mean concentration exceeds the CAAQS standard of 8.8 μg m^{-3} is reduced to approximately 0.0%. Similarly, removing emissions from Quebec, the RoC or the United States reduces the relative population of Quebec where the average concentration exceeds the WHO guideline of 5 μg m^{-3} to 0.0%, 85.8% or 66.8%, respectively.

These results suggest significant improvements in air quality in Quebec would be possible by controlling emissions only in Quebec. It is important to note that the model cell that contains the island of Montreal constitutes 0.2% of the area of Quebec, but contains 39.0% of the population of Quebec, and it is here that we find the greatest concentrations of several pollutants, including $PM_{2.5}$. In addition, there were forest fires in 2013 that

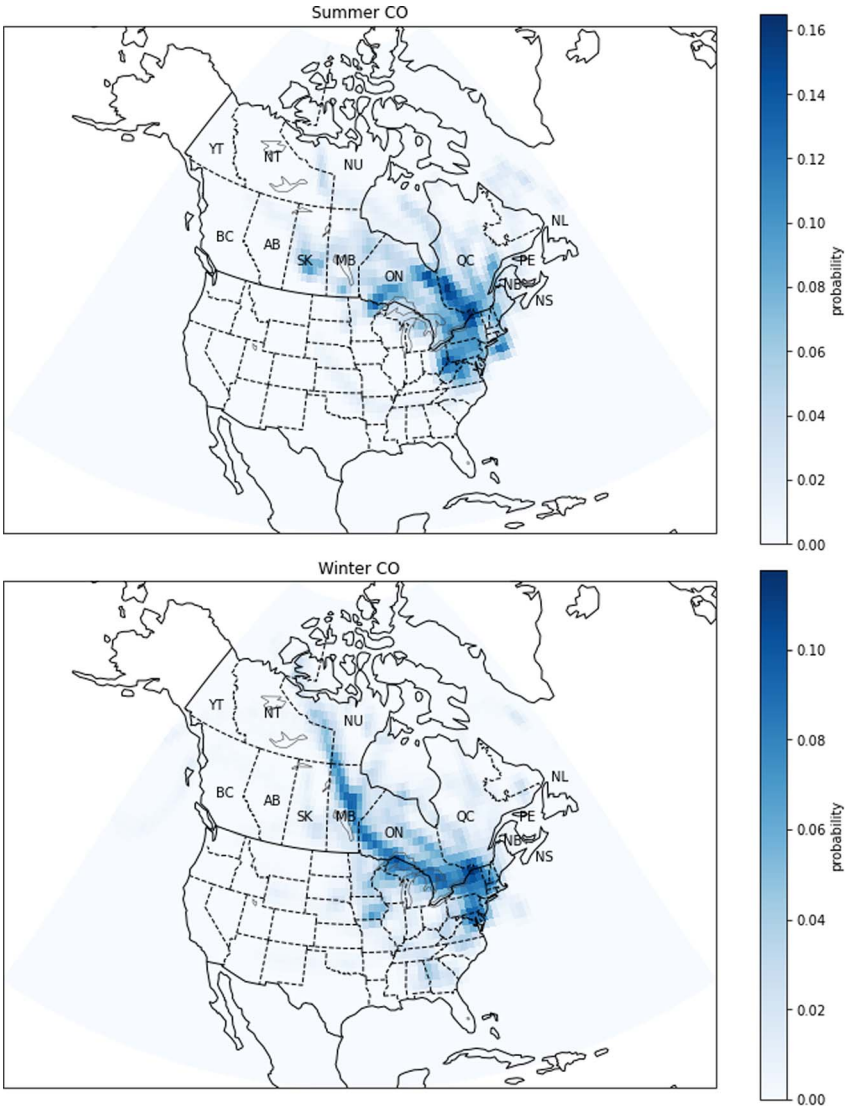

Fig. 13 Probability source contribution function maps calculated using the CO measurements. Top figure: summer probabilities. Bottom figure: winter probabilities. Canadian provinces and territories are labeled by postal abbreviation. NL: Newfoundland and Labrador, PE: Prince Edward Island, NS: Nova Scotia, NB: New Brunswick, QC: Quebec, ON: Ontario, MB: Manitoba, SK: Saskatchewan, AB: Alberta, BC: British Columbia, YT: Yukon, NT: Northwest Territories, NU: Nunavut.

caused a large area of Quebec to have elevated $PM_{2.5}$ concentrations, but affected principally regions with small populations.

We also performed the same analysis for SO_2 and NO_2, but the annual average concentrations were, in all cases, below the 2020 CAAQS thresholds (5.0 ppb for SO_2 and 17.0 ppb for NO_2), and even below the 2025 thresholds (4.0 ppb for SO_2 and 12.0 ppb for NO_2) everywhere. Among all the grid cells in Quebec, the maximum annual mean concentration of SO_2 in the base-case simulation was 2.48 ppb in 2012, and that of NO_2 was 6.73 ppb in 2012. Within Quebec, average NO_2 concentrations from 2012 to 2016 exceed the WHO threshold (10 μg m^{-3} NO_2, ≅5.2 ppb at normal temperature and pressure) in the cell covering the island of Montreal, and only in this grid cell, for all simulations except the noQC simulation. There is no WHO guideline for annual SO_2 concentrations. As our model evaluation showed a consistent low bias of about 50% in NO_x concentrations, we also compared against a NO_2 threshold of 2.6 ppb to account for this low bias. In the base-case simulation and the noRoC simulation, the grid cell just east of Montreal had a mean NO_2 concentration in excess of 2.6 ppb, bringing the population exposed to more than 2.6 ppb to 46.4% of Quebec's population. Otherwise, the results were identical to the comparison against a threshold of 5.2 ppb.

3.3 PSCF results

In the next section, we will discuss the results of the PSCF analysis. As there is frequently more variability between seasons in the spatial patterns of the PSCF maps than for the GEOS-Chem results, we present both summer and winter maps for each species in Fig. 10–15.

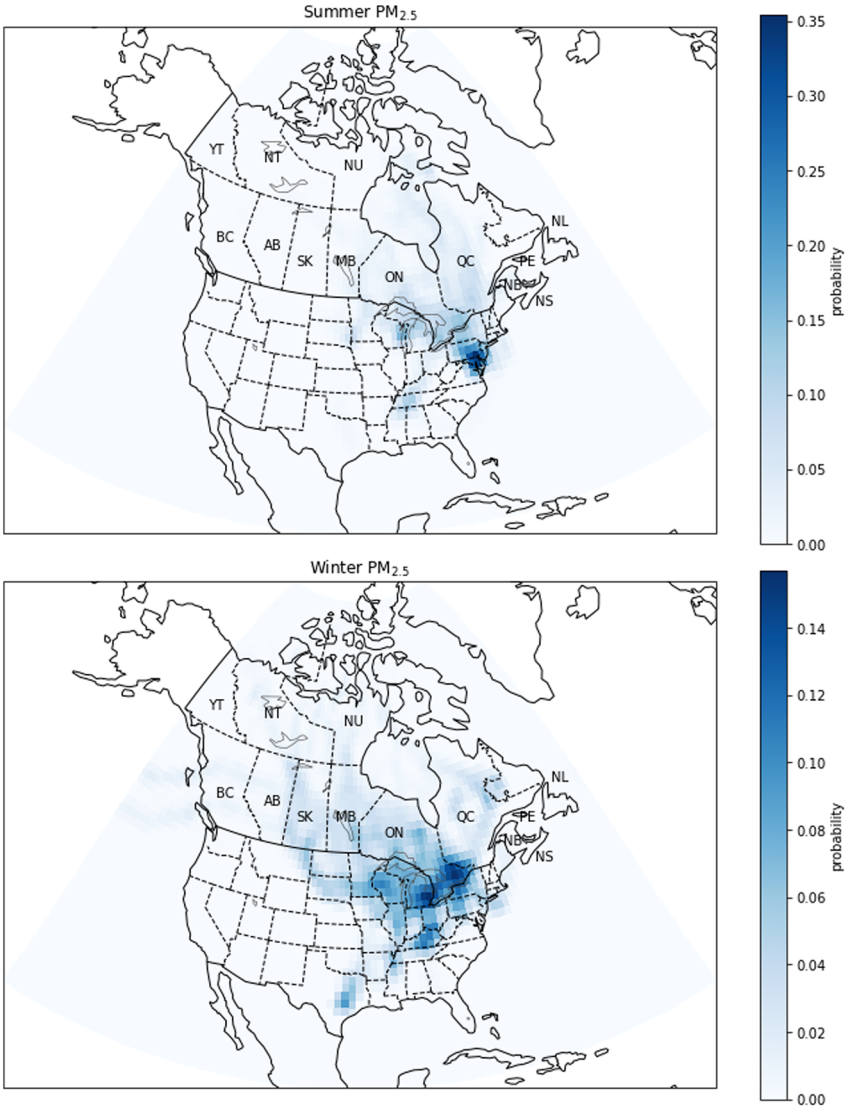

Fig. 14 Probability source contribution function maps calculated using the $PM_{2.5}$ measurements. Top figure: summer probabilities. Bottom figure: winter probabilities. Canadian provinces and territories are labeled by postal abbreviation. NL: Newfoundland and Labrador, PE: Prince Edward Island, NS: Nova Scotia, NB: New Brunswick, QC: Quebec, ON: Ontario, MB: Manitoba, SK: Saskatchewan, AB: Alberta, BC: British Columbia, YT: Yukon, NT: Northwest Territories, NU: Nunavut.

3.3.1 Gaseous pollutants. We begin this section by discussing the PSCF maps for the gaseous pollutants, specifically O_3. In summer, high concentrations of O_3 are most closely associated with back-trajectories that pass over the Greater Toronto Area and the East Coast of the United States (Fig. 10). These are both regions that would be expected to be source regions of NO_X from vehicular traffic and industry as well as anthropogenic VOC emissions, both of which would contribute to O_3 formation. We discuss the wintertime PSCF map in the supplement (Fig. A14†).

For NO_X, the PSCF calculations show a large difference between the potential sources in winter and in summer (Fig. 11). In summer, pollution comes from southern Quebec and areas south of Quebec such as the New York City metropolitan area. In winter, PSCF probabilities are highest in regions south of Quebec, specifically the east coast of the United States and major urban centers such as New York, Philadelphia and Washington. Although there are natural sources of NO_X such as biogenic emissions from soils, the GEOS-Chem simulations suggest most NO_X in urban centres is due to anthropogenic sources (Fig. 5). These urban anthropogenic sources would include vehicle exhaust. The increase in relative probability during winter in the United States compared to Quebec may be explained by the use of gas and oil heating in the United States, while in Quebec this type of heating is less important.[58–60]

In Quebec, SO_2 emissions come from aluminum production, industrial processes related to metallurgy and other minor sources.[61] PSCF calculations show differences, but also similarities in the regions of potential sources between winter and in summer (Fig. 12). In summer and winter, the high probabilities are mainly concentrated in southern Quebec, near the cities of Quebec and Montreal. At the same time, in winter, the

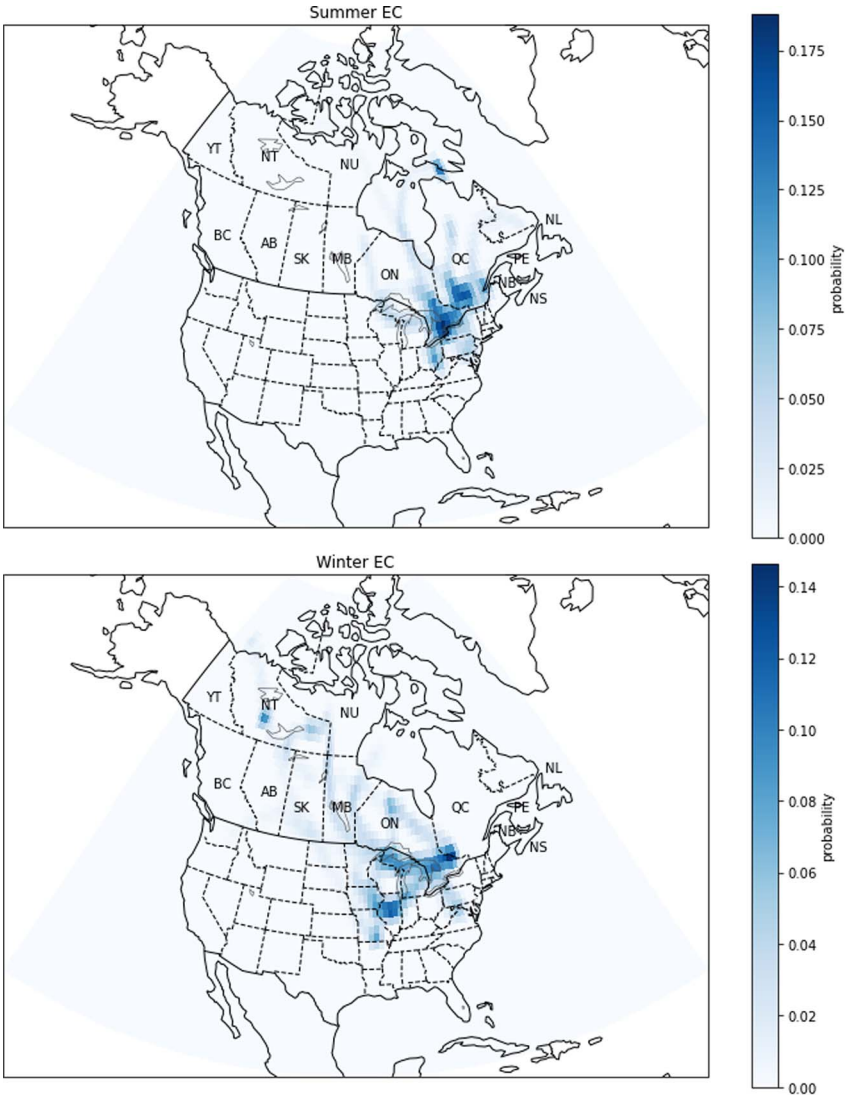

Fig. 15 Probability source contribution function maps calculated using the EC measurements. Top figure: summer probabilities. Bottom figure: winter probabilities. Canadian provinces and territories are labeled by postal abbreviation. NL: Newfoundland and Labrador, PE: Prince Edward Island, NS: Nova Scotia, NB: New Brunswick, QC: Quebec, ON: Ontario, MB: Manitoba, SK: Saskatchewan, AB: Alberta, BC: British Columbia, YT: Yukon, NT: Northwest Territories, NU: Nunavut.

intermediate probabilities extend over a larger region, including parts of the United States and Ontario, which is explained by the lifetime of SO_2 being longer in winter. This seasonal change is in agreement with GEOS-Chem simulations which showed that the relative differences between the base-case and the noCA or noUS simulations are greater in winter (Fig. A6 and A7†).

The largest CO emissions in Quebec come from the aluminum industry, including aluminum smelters in Bécancour (between Montreal and Québec City), Saguenay (north of Québec City) and Sept-Îles (on the north bank of the Gulf of St. Lawrence). Another important source of CO is vehicular combustion of fossil fuels. This means that major urban centers like New York and Toronto have high CO emissions. The PSCF calculations show a similarity between the regions of potential sources in winter and summer (Fig. 13). In summer, high probabilities are found in areas of southern Quebec, such as Montreal and Québec City. Regions south of Quebec, such as New York and southeastern Ontario, also have intermediate probabilities. In winter, PSCF probabilities are high in the same regions, but another area of high probabilities has emerged, which passes through southern Ontario and Manitoba. We have examined wildfire emissions for the winters of 2014–2016 according to the GFED4 inventory, and we did not find any large emissions that would explain this trajectory. We also note that large wildfires are not expected during the Canadian winter. We also examined possible sources in western Ontario, Manitoba, and the Northwest Territories from the National Pollutant Release Inventory (NPRI), and we did not find a clear and obvious source that explains this track. Due to the long atmospheric lifetime of CO, it is possible that this trajectory pathway is associated with long-range transport

across the Arctic, but it may instead be associated with a synoptic weather pattern that transports CO from the industrial region of southern Ontario or another more local source.

3.3.2 Particulate matter. For $PM_{2.5}$, PSCF calculations show a large difference between winter and summer in potential sources (Fig. 14). In summer, pollution comes from the regions south of Quebec, specifically the east coast of the United States and from major urban centers such as New York, Washington and Philadelphia. In winter, PSCF probabilities are highest in regions south-west of Quebec, including Ontario, Michigan and the US states around the Great Lakes. This is explained by the high emissions linked to human activities in these regions, for example the combustion of fuel and wood as well as emissions from the vehicle fleet. These sources would emit both primary aerosols such as soot as well as aerosol precursors such as volatile organic compounds and NO_X. There is also an intermediate probability in non-urban areas, including in Minnesota, Wisconsin, Illinois, Ohio and Kentucky. This observation is possibly explained by the high amount of ammonia emissions from agricultural activities in this region,[62] which form NH_4NO_3 aerosols. Colder winter temperatures favour the formation of aerosol NH_4NO_3,[63] yielding a greater impact on $PM_{2.5}$ concentrations if emissions are constant.

There are also seasonal differences in PSCF maps for EC (Fig. 15). The high probabilities are generally observed near large cities where there are sources of combustion emissions, for example vehicles. In summer, EC has high probabilities especially in the Greater Toronto Area, but there are also high probabilities in southwestern Quebec. Notably, in summer, the probabilities are close to zero in western and northern Canada indicating that there is not a strong contribution of forest fires to the EC concentration. At the same time, our confidence in this conclusion is limited by the sampling frequency which was 1 day in 3 or 1 day in 6, and it is therefore possible that there are smoke events which have not been captured by the measurements. On the other hand, in winter, the PSCF map shows a medium probability in the province of Ontario in an area close to the Quebec border, near Ottawa and Gatineau. Also, the map shows that the EC can come from the United States, more precisely from the Chicago area and the state of Illinois. The high-probability regions indicated by the PSCF analysis for $PM_{2.5}$ and EC show some consistency, particularly in winter when the probability is high in Ontario. This is expected as EC is a component of $PM_{2.5}$.

4. Discussion

Before comparing the results of the PSCF and GEOS-Chem analyses, it is important to note the different information provided by the two methods: our PSCF analysis isolates the periods with the highest concentrations of each pollutant, and determines the source regions of air masses during those periods, regardless of whether the source was natural or anthropogenic. On the other hand, the GEOS-Chem modelling results give contributions from anthropogenic sources from broad regions averaged over long periods. Natural sources may be highlighted by the PSCF analysis but not by the GEOS-Chem results. Also, a source with a significant but temporally-invariant contribution to pollutant concentrations would be highlighted by the GEOS-Chem analysis, but may be missed by the PSCF analysis.

Both GEOS-Chem and the PSCF results agree on an important role for emissions from the US on $PM_{2.5}$ concentrations, and in particular that the US is a relatively more important source region during the summer months. However, in winter, the PSCF results suggest a possible strong contribution from southern Ontario, while the GEOS-Chem results suggest that the US and Quebec are more important source regions than the rest of Canada (including southern Ontario). It is clear that $PM_{2.5}$ in Quebec is due to a variety of sources, but our analysis highlights the role of urban emissions from outside of Quebec. Both methods also show that local emissions contribute strongly to NO_X and SO_2 concentrations, with additional contributions from Ontario and the US, particularly in winter. These results suggest that local traffic emissions are likely the most important contributor to local NO_X concentrations, and local industry, including aluminum production and industrial processes related to metallurgy, is likely to be the most important contributor to local SO_2 concentrations.

Due to the predicted titration of O_3 in winter by anthropogenic emissions in the GEOS-Chem simulations, it is only meaningful to compare the GEOS-Chem and the PSCF results in summer. Both the PSCF and GEOS-Chem results show an important contribution of US emissions to O_3 concentrations. The PSCF analysis in particular highlights urban regions. This suggests that urban emissions of O_3 precursors from outside of Quebec, including vehicular NO_X and anthropogenic VOCs, are an important contributor to O_3 concentrations in the Quebec region.

Regarding CO, the GEOS-Chem and PSCF results agree about the importance of local and US emissions. We note that contributions to CO from forest fires and anthropogenic sources outside of North America would be included in the PSCF analysis but were not perturbed in the GEOS-Chem sensitivity simulations. However, the generally low percentage of CO attributable to anthropogenic emissions from any of the three regions in the GEOS-Chem results would be in agreement with a either a significant natural source of CO or long-range transport from outside of North America.

There is an apparent contrast in the GEOS-Chem and PSCF results for EC, with GEOS-Chem giving a greater importance to US emissions and the PSCF analysis showing a greater importance for sources in southern Ontario. However, we note that EC presents some special challenges when comparing the two analyses: EC was sampled less frequently and at fewer stations than the other pollutants. Also, forest fires are an important natural source of EC that would be highlighted by the PSCF analysis but not the GEOS-Chem analysis. We do not have reason to believe that there were large forest fires in southern Ontario during the study period, but air masses originating from forest fires may have traveled over southern Ontario before arriving at the measurement sites, leading to higher probabilities over southern Ontario. It is also possible that the emissions inventories used in GEOS-Chem underestimate EC from Canadian sources and/or overestimate EC from US sources.

5. Conclusions

We have investigated the sources of air pollution in Quebec through two complementary methods: back trajectory analysis using PSCF and chemical transport modelling. The PSCF analysis provides information on which source regions are best correlated with high-concentration events in Quebec, while the chemical transport modelling gives estimates of the contributions from three different source regions (Quebec, the rest of Canada (RoC), and the United States) to the concentrations of each of the investigated pollutants in Quebec.

The GEOS-Chem chemical transport modelling results reveal that all three regions considered have significant contributions to air pollutant concentrations in Quebec. For most pollutants, emissions from the RoC had a smaller contribution to concentrations in Quebec than local (Quebec) emissions or US emissions. Our results suggest that O_3 in summertime, when exceedances are expected to occur, is in a NO_X-limited regime in Quebec. We find that removing all anthropogenic emissions from any one of the three regions would reduce the fraction of the Quebec population living above the annual mean CAAQS $PM_{2.5}$ concentration threshold of 8.8 μg m^{-3} from 39.0% to about 0.0%. In contrast, only removal of emissions from Quebec decreases the fraction of the Quebec population living above the more stringent WHO $PM_{2.5}$ concentration threshold of 5.0 μg m^{-3} (from 87.7% to about 0.0%). While an absolute cessation of anthropogenic emissions is neither feasible nor desirable, our results suggest that significant improvements in air quality in Quebec would be possible through reductions in local emissions alone. At the same time, the achievable improvements will be limited by the strong transboundary contribution of certain pollutants, in particular for summertime O_3 for which the contribution from the United States exceeds that of Quebec.

The PSCF calculations show that there are a few regions associated with days of high concentrations of several pollutants. These regions include southern Quebec (local sources), the east coast of the United States, including the cities of New York, Washington and Philadelphia, and southeastern Ontario, including Toronto. Depending on the season, southern Quebec is associated with high concentrations of NO_X, SO_2, and CO; the east coast of the United States is associated with high concentrations of $PM_{2.5}$, NO_X, O_3, and CO; and southeastern Ontario is associated with high concentrations of $PM_{2.5}$ and EC.

The PSCF analysis relies on high-quality air pollutant measurements that are not strongly influenced by local sources. In contrast, several RSQAQ sites were specifically located with the intent of measuring local sources, making them less useful for this type of analysis. In addition, the RSQAQ stations are currently located in the southern portions of the province, predominantly along the St. Lawrence valley. This choice of placement allows for better understanding of the pollutant exposure in the most populous region of Quebec, but limits our ability to evaluate pollutant transport to the northern regions of the province.

The two methods provided some contrasting results regarding the sources of CO and EC in Quebec. This is potentially due to the fact that we did not perturb natural emissions in the GEOS-Chem simulations, including forest fires, which would influence the PSCF analysis. The smaller number of stations and the less frequent sampling of EC is also a source of greater uncertainty in the PSCF analysis. However, both methods highlight the importance of local emissions for NO_X and SO_2 concentrations, non-Quebec sources for summertime O_3 concentrations, and an important contribution from US emissions to $PM_{2.5}$ concentrations in Quebec.

Author contributions

PH provided conceptualization and funding acquisition. RS, NT, and HR performed the chemical transport modelling and analysis, and CP performed the PSCF modelling and analysis. RS wrote the original draft with input from PH and CP, and all authors reviewed the text.

Conflicts of interest

There are no conflicts to declare.

Acknowledgements

We would like to thank James King of the Université de Montréal and Hélène Côté and Biljana Music or Ouranos for thoughtful discussions about this work. This work was supported by the Ministère de l'Environnement, de la Lutte contre les changements climatiques, de la Faune et des Parcs du Québec. This research was enabled in part by support provided by Cacul Québec (**https://calculquebec.ca**) and the Digital Research Alliance of Canada (**https://alliancecan.ca**). NT acknowledges financial support from the Natural Sciences and Engineering Research Council of Canada through the Undergraduate Student Research Awards program.

Notes and references

1 C. A. Pope and D. W. Dockery, *J. Air Waste Manage. Assoc.*, 2006, **56**, 709–742.
2 C. A. Pope, M. Ezzati and D. W. Dockery, *N. Engl. J. Med.*, 2009, **360**, 376–386.
3 F. Laden, J. Schwartz, F. E. Speizer and D. W. Dockery, *Am. J. Respir. Crit. Care Med.*, 2006, **173**, 667–672.
4 D. M. Stieb, S. Judek and R. T. Burnett, *J. Air Waste Manag. Assoc.*, 2002, **52**, 470–484.
5 D. R. Reidmiller, A. M. Fiore, D. A. Jaffe, D. Bergmann, C. Cuvelier, F. J. Dentener, B. N. Duncan, G. Folberth, M. Gauss, S. Gong, P. Hess, J. E. Jonson, T. Keating, A. Lupu, E. Marmer, R. Park, M. G. Schultz, D. T. Shindell, S. Szopa, M. G. Vivanco and A. Zuber, *Atmos. Chem. Phys.*, 2009, **9**, 5027–5042.
6 J. M. Kelly, E. A. Marais, G. Lu, J. Obszynska, M. Mace, J. White and R. J. Leigh, *City Environ. Interact.*, 2023, **18**, 100100.
7 U. Jeong, J. Kim, H. Lee and Y. G. Lee, *Atmos. Environ.*, 2017, **150**, 33–44.

8 S. C. Anenberg, J. J. West, H. Yu, M. Chin, M. Schulz, D. Bergmann, I. Bey, H. Bian, T. Diehl, A. Fiore, P. Hess, E. Marmer, V. Montanaro, R. Park, D. Shindell, T. Takemura and F. Dentener, *Air Qual. Atmos. Health*, 2014, **7**, 369–379.
9 Q. Liang, R. S. Stolarski, S. R. Kawa, J. E. Nielsen, A. R. Douglass, J. M. Rodriguez, D. R. Blake, E. L. Atlas and L. E. Ott, *Atmos. Chem. Phys.*, 2010, **10**, 2269–2286.
10 F. Dentener, T. Keating, H. Akimoto, N. Pirrone, S. Dutchak and A. Zuber, Convention on Long-range Transboundary Air Pollution. Task Force on Hemispheric Transport of Air Pollution, United Nations Economic Commission for Europe and UNECE Task Force on Emission Inventories and Projections, *Hemispheric Transport of Air Pollution 2010: Part A – Ozone and Particulate Matter (Air Pollution Studies)*, United Nations, New York, Illustrated, 2011.
11 Ville de Montréal Service de l'environnement, *Environmental Assessment Report (EAR) 2022 Air Quality in Montréal, Division de la planification et du suivi environnemental*, Montréal, Québec, Canada, 2023.
12 Gouvernement de Québec, Ministère de l'Environnement, de la Lutte contre les changements climatiques and de la Faune et des Parcs, *Statistiques annuelles de l'IQA*, 2021, **https://www.iqa.environnement.gouv.qc.ca/contenu/grille_stat_jour.asp?annee=2021**, accessed July 20, 2023.
13 R. Vet and C.-U. Ro, *Atmos. Environ.*, 2008, **42**, 2518–2529.
14 Q. Li, D. J. Jacob, R. Park, Y. Wang, C. L. Heald, R. Hudman, R. M. Yantosca, R. V. Martin and M. Evans, *J. Geophys. Res.*, 2005, **110**, D10301.
15 E. Chan and R. J. Vet, *Atmos. Chem. Phys.*, 2010, **10**, 8629–8647.
16 T. Zhang, Y. Chen, R. Tan and X. Xu, *Atmosphere*, 2021, **12**, 1300.
17 J. Meng, R. V. Martin, C. Li, A. van Donkelaar, Z. A. Tzompa-Sosa, X. Yue, J.-W. Xu, C. L. Weagle and R. T. Burnett, *Environ. Sci. Technol.*, 2019, **53**, 10269–10278.
18 L. G. Chestnut and D. M. Mills, *J. Environ. Manage.*, 2005, **77**, 252–266.
19 J. Dupont, *La problématique des lacs acides au Québec, Direction du suivi de l'état de l'environnement*, Ministère de l'Environnement, 2004.
20 L. J. Mickley, D. J. Jacob, B. D. Field and D. Rind, *Geophys. Res. Lett.*, 2004, **31**, L24103.
21 M. Crippa, D. Guizzardi, T. Butler, T. Keating, R. Wu, J. Kaminski, J. Kuenen, J. Kurokawa, S. Chatani, T. Morikawa, G. Pouliot, J. Racine, M. D. Moran, Z. Klimont, P. M. Manseau, R. Mashayekhi, B. H. Henderson, S. J. Smith, H. Suchyta, M. Muntean and K. Foley, *Earth Syst. Sci. Data*, 2023, **15**, 2667–2694.
22 R. M. Hoesly, S. J. Smith, L. Feng, Z. Klimont, G. Janssens-Maenhout, T. Pitkanen, J. J. Seibert, L. Vu, R. J. Andres, R. M. Bolt, T. C. Bond, L. Dawidowski, N. Kholod, J. Kurokawa, M. Li, L. Liu, Z. Lu, M. C. P. Moura, P. R. O'Rourke and Q. Zhang, *Geosci. Model Dev.*, 2018, **11**, 369–408.
23 *Gouvernement du Québec – Ministère de l'Environnement et de la Lutte contre les changements climatiques, Réseau de surveillance de la qualité de l'air du Québec*, **https://www.environnement.gouv.qc.ca/air/reseau-surveillance/Carte.asp**, accessed August 18, 2022.
24 I. Bey, D. J. Jacob, R. M. Yantosca, J. A. Logan, B. D. Field, A. M. Fiore, Q. Li, H. Y. Liu, L. J. Mickley and M. G. Schultz, *J. Geophys. Res.*, 2001, **106**, 23073–23095.
25 R. J. Park, D. J. Jacob, B. D. Field, R. M. Yantosca and M. Chin, *J. Geophys. Res.*, 2004, **109**, D15204.
26 S. D. Eastham, M. S. Long, C. A. Keller, E. Lundgren, R. M. Yantosca, J. Zhuang, C. Li, C. J. Lee, M. Yannetti, B. M. Auer, T. L. Clune, J. Kouatchou, W. M. Putman, M. A. Thompson, A. L. Trayanov, A. M. Molod, R. V. Martin and D. J. Jacob, *Geosci. Model Dev.*, 2018, **11**, 2941–2953.
27 G. Luo, F. Yu and J. M. Moch, *Geosci. Model Dev.*, 2020, **13**, 2879–2903.
28 G. Luo, F. Yu and J. Schwab, *Geosci. Model Dev.*, 2019, **12**, 3439–3447.
29 P. K. Hopke, *J. Air Waste Manag. Assoc.*, 2016, **66**, 237–259.
30 A. F. Stein, R. R. Draxler, G. D. Rolph, B. J. B. Stunder, M. D. Cohen and F. Ngan, *Bull. Amer. Meteor. Soc.*, 2015, **96**, 2059–2077.
31 I. Pisso, E. Sollum, H. Grythe, N. I. Kristiansen, M. Cassiani, S. Eckhardt, D. Arnold, D. Morton, R. L. Thompson, C. D. Groot Zwaaftink, N. Evangeliou, H. Sodemann, L. Haimberger, S. Henne, D. Brunner, J. F. Burkhart, A. Fouilloux, J. Brioude, A. Philipp, P. Seibert and A. Stohl, *Geosci. Model Dev.*, 2019, **12**, 4955–4997.
32 J. C. Lin, *J. Geophys. Res.*, 2003, **108**, ACH2.
33 Canadian Council of Ministers of the Environment, *Ambient Air Monitoring and Quality Assurance/Quality Control Guidelines, National Air Pollution Surveillance Program*, **https://ccme.ca/en/res/ambientairmonitoringandqa-qcguidelines_ensecure.pdf**, accessed August 24, 2022.
34 L. L. Ashbaugh, W. C. Malm and W. Z. Sadeh, *Atmos. Environ.*, 1985, **19**, 1263–1270.
35 Y. Zeng and P. K. Hopke, *Atmos. Environ.*, 1989, **23**, 1499–1509.
36 M. Kanamitsu, *Weather Forecasting*, 1989, **4**, 335–342.
37 J. E. Petit, O. Favez, A. Albinet and F. Canonaco, *Environ. Model. Software*, 2017, **88**, 183–187.
38 F. Shen, L. Zhang, L. Jiang, M. Tang, X. Gai, M. Chen and X. Ge, *Environ. Int.*, 2020, **137**, 105556.
39 Y. Yuan, X. Zhang, J. Zhao, F. Shen, D. Nie, B. Wang, L. Wang, M. Xing and M. I. Hegglin, *Front. Public Health*, 2023, **11**, 1075262.
40 S. S. Raj, O. O. Krüger, A. Sharma, U. Panda, C. Pöhlker, D. Walter, J. Förster, R. P. Singh, T. Klimach, E. Darbyshire, S. T. Martin, G. McFiggans, H. Coe, J. Allan, V. K. Soni, H. Su, M. O. Andreae, U. Pöschl and S. S. Gunthe, *J. Geophys. Res.*, 2021, **126**, e2021JD035681.
41 L. Giglio, J. T. Randerson and G. R. van der Werf, *J. Geophys. Res. Biogeosci.*, 2013, **118**, 317–328.
42 US EPA, *2016v1 Air Emissions Modeling Platform*, **https://www.epa.gov/air-emissions-modeling/2016v1-platform**, accessed May 2, 2023.
43 M. E. J. Stettler, S. Eastham and S. R. H. Barrett, *Atmos. Environ.*, 2011, **45**, 5415–5424.

44 N. W. Simone, M. E. J. Stettler and S. R. H. Barrett, *Transport. Res. Transport Environ.*, 2013, **25**, 33–41.
45 R. F. Silvern, D. J. Jacob, L. J. Mickley, M. P. Sulprizio, K. R. Travis, E. A. Marais, R. C. Cohen, J. L. Laughner, S. Choi, J. Joiner and L. N. Lamsal, *Atmos. Chem. Phys.*, 2019, **19**, 8863–8878.
46 M. J. Cooper, R. V. Martin, C. A. McLinden and J. R. Brook, *Environ. Res. Lett.*, 2020, **15**, 104013.
47 L. M. Judd, J. A. Al-Saadi, S. J. Janz, M. G. Kowalewski, R. B. Pierce, J. J. Szykman, L. C. Valin, R. Swap, A. Cede, M. Mueller, M. Tiefengraber, N. Abuhassan and D. Williams, *Atmos. Meas. Tech.*, 2019, **12**, 6091–6111.
48 S. K. Kharol, R. V. Martin, S. Philip, B. Boys, L. N. Lamsal, M. Jerrett, M. Brauer, D. L. Crouse, C. McLinden and R. T. Burnett, *Atmos. Environ.*, 2015, **118**, 236–245.
49 P. S. Kim, D. J. Jacob, J. A. Fisher, K. Travis, K. Yu, L. Zhu, R. M. Yantosca, M. P. Sulprizio, J. L. Jimenez, P. Campuzano-Jost, K. D. Froyd, J. Liao, J. W. Hair, M. A. Fenn, C. F. Butler, N. L. Wagner, T. D. Gordon, A. Welti, P. O. Wennberg, J. D. Crounse and A. E. Perring, *Atmos. Chem. Phys.*, 2015, **15**, 10411–10433.
50 K. R. Travis and D. J. Jacob, *Geosci. Model Dev.*, 2019, **12**, 3641–3648.
51 Y. Li, R. V. Martin, C. Li, B. L. Boys, A. van Donkelaar, J. Meng and J. R. Pierce, *Atmos. Chem. Phys.*, 2023, **23**, 12525–12543.
52 D. D. Parrish, K. S. Law, J. Staehelin, R. Derwent, O. R. Cooper, H. Tanimoto, A. Volz-Thomas, S. Gilge, H. E. Scheel, M. Steinbacher and E. Chan, *Geophys. Res. Lett.*, 2013, **40**, 1631–1636.
53 H. Bowman, S. Turnock, S. E. Bauer, K. Tsigaridis, M. Deushi, N. Oshima, F. M. O'Connor, L. Horowitz, T. Wu, J. Zhang, D. Kubistin and D. D. Parrish, *Atmos. Chem. Phys.*, 2022, **22**, 3507–3524.
54 J. A. Fisher, D. J. Jacob, M. T. Purdy, M. Kopacz, P. Le Sager, C. Carouge, C. D. Holmes, R. M. Yantosca, R. L. Batchelor, K. Strong, G. S. Diskin, H. E. Fuelberg, J. S. Holloway, E. J. Hyer, W. W. McMillan, J. Warner, D. G. Streets, Q. Zhang, Y. Wang and S. Wu, *Atmos. Chem. Phys.*, 2010, **10**, 977–996.
55 *Le conseil canadien des ministres de l'environnement, Qualité de l'air*, **https://www.ccme.ca/fr/qualite-de-lair#slide-7**, accessed May 2, 2023.
56 World Health Organization, *WHO Global Air Quality Guidelines: Particulate Matter (PM2.5 and PM10), Ozone, Nitrogen Dioxide, Sulfur Dioxide and Carbon Monoxide*, Geneva, 2021.
57 Agriculture and Agri-Food Canada, *Population of Canada, 10km Gridded - Open Government Portal*, **https://open.canada.ca/data/en/dataset/c6c48391-fd2f-4d8a-93c8-eb74f58a859b**, accessed May 9, 2023.
58 *Gouvernement du Québec - Ministère de l'Énergie et des Ressources naturelles*, Gaz naturel, **https://mern.gouv.qc.ca/energie/hydrocarbures/gaz-naturel/**, accessed June 27, 2022.
59 U.S. Energy Information Administration, *Use of energy explained - Energy use in homes*, **https://www.eia.gov/energyexplained/use-of-energy/homes.php**, accessed June 27, 2022.
60 J. Whitmore and P.-O. Pineau, *État de l'énergie au Québec 2019, Chaire de gestion du secteur de l'énergie, HEC Montréal, préparé pour Transition énergétique Québec*, Montréal, 2018.
61 Government of Canada, *National Pollutant Release Inventory Dashboard*, **https://www.canada.ca/en/environment-climate-change/services/national-pollutant-release-inventory/tools-resources-data/all-year-dashboard.html**, accessed June 27, 2022.
62 L. Liu, W. Xu, X. Lu, B. Zhong, Y. Guo, X. Lu, Y. Zhao, W. He, S. Wang, X. Zhang, X. Liu and P. Vitousek, *Proc. Natl. Acad. Sci. U.S.A.*, 2022, **119**, e2121998119.
63 M. Mozurkewich, *Atmos. Environ. Part A Gen. Top.*, 1993, **27**, 261–270.